

## Effective critical and tricritical exponents

Eberhard K. Riedel\*

*Department of Physics, Duke University, Durham, North Carolina 27706*

Franz J. Wegner

*Institut für Festkörperforschung, KFA Jülich, D517 Jülich, Germany*

(Received 13 July 1973)

A semi-microscopic scaling-field theory is developed for crossover phenomena near critical and tricritical points. The theory is based on a renormalization-group description of a model with two competing fixed points (such as a critical and a tricritical fixed point) in terms of scaling fields. The coupled nonlinear differential equations for scaling fields are truncated such as to preserve the physics essential for crossover phenomena. The approach allows the explicit calculation of thermodynamic functions for (i) tricritical systems and (ii) critical systems with an irrelevant scaling field. We obtain, for example, an explicit expression for the scaling function of the susceptibility, which describes the crossover from the tricritical to the critical region. The idea of "flow diagrams" in the scaling-field space is used to characterize crossover phenomena globally in the whole critical region. The concept of asymptotic critical exponents is generalized and effective critical exponents are introduced as logarithmic derivatives of thermodynamic quantities with respect to experimental fields and scaling fields, respectively. By using the method of effective exponents the size of the crossover region between regions of different asymptotic critical behavior is estimated. For the susceptibility, the width of the crossover region in decades of the effective temperature variable is roughly equal to the inverse of the crossover exponent. In the case of a critical system with a slow transient the asymptotic critical exponent is only reached extremely close to the critical point (unless the amplitude of the transient vanishes). It might then be impossible to determine the asymptotic exponent experimentally or by conventional series-expansion techniques, and an analysis of the data in terms of effective exponents is the alternative. The scaling-field approach is applied to three systems with crossover phenomena: (i) the model for tricritical systems with molecular-field tricritical exponents, (ii) the Ashkin-Teller model in three dimensions, and (iii) a model for phase transitions with Fisher exponent renormalization due to a constraint.

### I. INTRODUCTION

Critical exponents characterize the way in which various physical quantities diverge to infinity or converge to zero as the temperature, or other variable, approaches its critical-point value. The critical exponent  $\lambda$  of a function  $f(\mu)$  varying as  $\mu^\lambda$  when  $\mu$  approaches zero from above is defined<sup>1</sup> as  $\lambda = \lim_{\mu \rightarrow 0^+} \{\ln f(\mu) / \ln \mu\}$ . This definition has two disadvantages. (i) It carries the hidden question in it, both experimentally and theoretically, of the size of the critical region in which one will be able to see the true asymptotic value of the exponent. (ii) It cannot be easily applied to phase transitions with crossover phenomena, where in different areas of the critical region different "asymptotic" forms govern the approach to criticality. In this article<sup>2</sup> we introduce the concept of *effective critical exponents*. They provide a *local* measure for the degree of singularity of physical quantities in the critical region. The effective critical exponent of a function  $f(\mu)$  is defined by the logarithmic derivative  $\lambda_{\text{eff}}(\mu) = d \ln f(\mu) / d \ln \mu$ . It coincides in the limit  $\mu \rightarrow 0^+$  with the *asymptotic* critical exponent, i. e.,  $\lambda = \lim_{\mu \rightarrow 0^+} \{\lambda_{\text{eff}}(\mu)\}$ . Effective critical exponents as functions of the number of terms in series expansions are also discussed.

The second major purpose of this article is to develop further the *scaling-field approach* to critical phenomena by the authors. This method is used to study the behavior of effective critical exponents, and to calculate scaling functions for systems with crossover phenomena. The investigations are based on a renormalization-group<sup>3-5</sup> model with two fixed points, such as a tricritical fixed point and a critical fixed point, that is defined by a set of differential equations for three "scaling fields." The scaling fields considered depend on three experimental fields: the temperature, a nonordering field, and an ordering field. The model describes (a) the competition between the tricritical and the critical behavior in the neighborhood of a critical line which terminates in a tricritical point and (b) the effects of an irrelevant field (or operator) on the critical behavior near a critical point. We apply the model to three systems with crossover phenomena: (i) a tricritical model with molecular-field tricritical exponents,<sup>6-9</sup> (ii) the Ashkin-Teller model in three dimensions,<sup>10-12</sup> and (iii) a model for phase transitions with Fisher exponent renormalization due to a constraint.<sup>13</sup> The differential equations for the scaling fields of the model are truncated such as to preserve the essential physics of crossover

phenomena. The asymptotic critical exponents entering these equations as parameters are assumed to be known. The advantage of defining models in terms of scaling-field equations is that they can be kept sufficiently simple to be exactly soluble, but still be made sophisticated enough to include nonlinear features like crossover phenomena,<sup>14-16</sup> which so far could not be studied microscopically. A derivation of the differential equations for scaling fields starting from a Hamiltonian definition of the model is considered a separate problem that is not discussed here. The renormalization-group theory provides, in a general form, the relation between the Hamiltonian approach and the scaling-field approach.<sup>3,7</sup> The elements of the renormalization-group description of critical phenomena and the concept of scaling fields are presented in Sec. II. In Sec. III nonlinear scaling-field equations defining the models discussed in this article are introduced and briefly analyzed. These equations constitute the basis for the investigations in the following sections.

In Sec. IV we calculate for this model thermodynamic functions near criticality. Their scaling properties are found to agree with the predictions of our scaling theory for crossover phenomena (including the double-scaling feature)<sup>14,17</sup> Moreover, explicit expressions for the *scaling functions* are obtained. Also in Sec. IV "flow diagrams" in the scaling-field space representing the development of states generated by the renormalization-group equations are discussed. Flow diagrams give a clear over-all picture of crossover phenomena in the whole critical region. Then, in Sec. V, effective critical exponents are derived that depend on the asymptotic critical exponents and the scaling fields (and via those on the experimental fields). It is found that the width of the crossover region separating tricritical and critical-line regimes depends crucially on the value of the crossover exponent  $\phi$ .<sup>14</sup> For the susceptibility the crossover occurs gradually over about  $1/\phi$  decades, in units of the relative distance to the critical line. For a tricritical system with molecular-field-like tricritical exponents<sup>6,7</sup> the width of the crossover region is of the order of  $10^2$ . For the three-dimensional Ashkin-Teller model,<sup>18</sup> which exhibits a tricritical point with Ising-like tricritical exponents, the width is of the order of  $10^9$ . This result shines new light on the observability of crossover phenomena and the universality principle. Another group of crossover phenomena occurs in phase transitions subject to a constraint which show the Fisher exponent renormalization.<sup>13</sup> In Sec. VI it is shown that this crossover is also characterized by the set of differential equations defined in Sec. III. Therefore, all results of Secs. IV and V apply to this case,

of course, subject to a redefinition of the critical exponents and scaling fields. The width of the region over which the Fisher exponent renormalization occurs is, for the decorated Ising model,<sup>13,19</sup> of the order of  $10^6$ .

Series-expansion techniques have played an important role for estimating critical exponents.<sup>1</sup> For systems with crossover phenomena (with small  $\phi$ ) and systems with slow transients, it is difficult to extrapolate relatively short series to obtain the true asymptotic exponents. To investigate this question we discuss in Sec. VII effective critical exponents as functions of the number  $n$  of terms included in series expansions. We find a weak dependence of the effective critical exponents on the number of terms in the form of a power law with an exponent given roughly by the crossover exponent. For the three-dimensional Ashkin-Teller model, for example, the difference between the effective and the asymptotic critical exponent decays like  $n^{-0.09}$ . This explains the difficulties recently encountered in a series-expansion test<sup>18</sup> of the universality principle for this model.

The scaling-field method provides a simple and powerful technique for studying nonlinear effects in the theory of critical phenomena. In particular, the approach allows the extension of the description of critical phenomena into the *whole* critical region. We emphasize that we have solved only the most simplified example of a set of scaling-field equations describing the competition between different fixed points (i. e., different critical instabilities). A number of modifications, some of which are described in Secs. III C, VII C, and Appendix B, are needed to describe realistic systems with crossover phenomena. However, we would like to suppose that our approach has succeeded in including some of the essential physics of crossover phenomena.

## II. UNIFIED SCALING APPROACH TO CRITICAL PHENOMENA

The renormalization-group procedure<sup>3,5,20</sup> leads to a microscopic definition of the variables in which thermodynamic quantities near criticality are homogeneous.<sup>4,6,7</sup> These scaling variables, which are related to geometrical features of the phase diagram of the system, are called scaling fields [compare Eqs. (2.3) and (2.4) below].<sup>6,17,21</sup> The scaling-field method, as developed in this and a previous publication,<sup>7</sup> allows one to analyze the form of thermodynamic quantities near criticality and to evaluate scaling functions in terms of the scaling fields. In this section we review briefly the renormalization-group procedure and the scaling-field method. The following sections will show the scaling-field approach "at work." (Further details on this method can be found in Refs. 4 and 7.)

The Wilson renormalization-group procedure defines a sequence of effective Hamiltonians  $H_l$ . We denote the renormalization-group operation that is related to a change in the length scale by a factor  $e^l$  by  $R^l$ . The sequence of effective Hamiltonians  $H_l$  is obtained by applying the transformation  $R^l$  to the initial Hamiltonian  $H_0$ ,

$$H_l = R^l H_0 . \quad (2.1)$$

(Implicit in  $H_0$  is the factor  $\beta = 1/k_B T$ .) The operation  $R^l$  is defined to leave the partition function of the system invariant. Depending on the choice of  $R^l$  the operation has group or semigroup properties,<sup>22</sup> but, in any case, it satisfies  $R^l R^{l'} = R^{l+l'}$  for positive  $l$  and  $l'$ . If the initial Hamiltonian is the critical Hamiltonian  $H_{0,c}$  then the limit

$$\lim_{l \rightarrow \infty} H_{l,c} = \lim_{l \rightarrow \infty} R^l H_{0,c} = H^* \quad (2.2)$$

tends to a fixed-point Hamiltonian  $H^*$ . Each critical Hamiltonian is associated with a fixed point. The basic idea of the renormalization-group approach is that at criticality the effective Hamiltonians  $H_{l,c}$  become asymptotically invariant under changes of the length scale of the system.

Let us describe the deviations of  $H_l$  from the fixed point  $H^*$  by an expansion into a complete set of operators  $Q_i$ ,

$$H_l = H^* + \sum_i \mu_i(l) Q_i . \quad (2.3)$$

Then the thermodynamic potential  $F$  per unit volume satisfies the generalized scaling relation

$$F\{\mu_i(0)\} = e^{-dl} F\{\mu_i(l)\} . \quad (2.4)$$

(The scale factor  $e^{-dl}$  is a consequence of the extension of the  $d$ -dimensional reference volume under the scale transformation.  $F$  also includes a factor  $\beta = 1/k_B T$ .) For the description of critical phenomena it is useful to choose the  $Q_i$  such that the equations of motion for the  $\mu_i$  decouple in linear order in  $\mu_i$ ,

$$\frac{\partial \mu_i(l)}{\partial l} = y_i \mu_i(l) + O(\mu_i^2) . \quad (2.5)$$

With this approximation Eq. (2.3) yields

$$R^l H_0 = H^* + \sum_i \mu_i(0) e^{y_i l} Q_i + O(\mu_i^2) , \quad (2.6)$$

and Eq. (2.4) assumes in this asymptotic critical region the conventional scaling form [however, with the usual scaling variables  $\tau = (T - T_c)/T_c$ , etc., replaced by the "fields"  $\mu_i$ ]. The scaling indices  $y_i$  are related to the ordinary asymptotic critical exponents. The fields  $\mu_i(l)$  are termed scaling fields and the conjugate densities  $Q_i$  scaling densities. In the following we adopt the convention of denoting the initial scaling fields  $\mu_i(l=0)$  by  $\mu_i$ .

All information about the critical behavior of the

system is contained in the scaling fields. The scaling relation (2.4) connects the values of  $F$  in the two states  $\{\mu_i(0)\}$  and  $\{\mu_i(l)\}$ . This fact is used to evaluate effective critical exponents and scaling functions in the following sections. The idea is to choose the state  $\{\mu_i(l)\}$  outside the critical region, where one can calculate  $F$  by conventional techniques, and calculate  $F$  in the critical region at  $\{\mu_i(0)\}$  by determining the scale parameter  $l$  that connects the two states. The idea applies analogously to the evaluation of any other thermodynamic quantity.

In general one has to consider nonlinear contributions to the derivatives of the scaling fields  $\mu_i(l)$  in Eq. (2.5) and, therefore, to start from the set of coupled scaling-field equations<sup>23</sup>

$$\begin{aligned} \frac{\partial \mu_i(l)}{\partial l} = & y_i \mu_i(l) \\ & + \frac{1}{2} \sum_{j,k} a_{ijk} \mu_j(l) \mu_k(l) + \dots \end{aligned} \quad (2.7)$$

The nonlinear terms lead to a number of corrections to the asymptotic power-law behavior near critical points. The most prominent examples are logarithmic singularities. (In particular, if the critical exponent  $2 - \alpha$  of the free energy is an integer an additional logarithmic factor appears in the specific heat.<sup>4</sup> Even noninteger powers of logarithmic corrections occur at critical points in four dimensions and tricritical points in three dimensions, where certain other exponent relations are satisfied.<sup>7</sup>) Other effects due to the coupling of irrelevant and relevant scaling fields give rise to additive corrections to the asymptotically dominant critical behavior ("confluent singularities"<sup>24</sup>), and are further discussed in Sec. IV. Quite generally, the relative importance of the linear term and the nonlinear terms in Eq. (2.7) determines "where" in the critical region the crossover between apparently different critical behavior occurs.

If the critical behavior of a system is determined by several fixed points then the quadratic terms in the scaling-field equations of motion (2.7) describe the effects of their competition in leading order. (This statement becomes incorrect when the fixed points are not close to each other.)

Therefore, we may use equations of the general form (2.7) to analyze crossover phenomena due to the competition between two fixed points as they occur in weakly anisotropic systems<sup>14</sup> (spin anisotropy, lattice anisotropy, etc.), and in systems near tricritical points.<sup>17</sup> In the following we define a model for systems with competing critical and tricritical phase transitions in terms of differential equations for scaling fields. We will assume that all asymptotic critical exponents are known and construct the simplest model exhibiting cross-

over phenomena for these given exponents. The latter assumption is insignificant for our purposes. The essential point is that we are interested in the values of the effective critical exponents *relative* to the asymptotic ones, and in the explicit form of the scaling functions for systems with crossover phenomena.

### III. MODEL

In this section we formulate in terms of differential equations for scaling fields a model for a system with competing critical and tricritical phase transitions.

#### A. Scaling-field equations

We assume that the thermodynamic state of the model system can be characterized by a set of three scaling fields  $(\mu_1, \mu_2, \mu_h)$ .<sup>6,7</sup> Here  $\mu_h$  denotes the symmetry-breaking field (ordering field) which is conjugate to the order parameter. The field  $\mu_1$  describes the departure of the state of the system from the critical line (i. e., the line of second-order critical points), and along the critical line the field  $\mu_2$  (nonordering field) measures the distance from the tricritical point. Therefore, all three fields have to vanish at the tricritical fixed point, whereas at the critical fixed point only  $\mu_1$  and  $\mu_h$  have to vanish. We note that the whole critical line is described by one fixed point [compare Eq. (3.19)]. Since we are free to choose the scale for  $\mu_2$  we choose  $\mu_2=1$  for the critical fixed point. Then our model will be constructed such that it has the two fixed points

$$(\mu_1^*, \mu_2^*, \mu_h^*) = \begin{cases} (0, 0, 0), & \text{tricritical fixed point} \\ (0, 1, 0), & \text{critical fixed point.} \end{cases} \quad (3.1)$$

In Fig. 1 these two fixed points are represented in the scaling-field space  $(\mu_1, \mu_2, \mu_h)$ .

Next we define the equations of motion for the scaling fields. Asymptotically close to the tricritical fixed point and the critical fixed point, respectively, the equations for  $\mu_1$  are linear,

$$\frac{\partial \mu_1(l)}{\partial l} = y_{1t} \mu_1(l) \quad \text{and} \quad \frac{\partial \mu_1(l)}{\partial l} = y_{1c} \mu_1(l), \quad (3.2)$$

with  $d/y_{1c,1t} = 2 - \alpha_{c,t}$ . The simplest way to obtain an equation that covers both limits (3.2) is to use the interpolation formula

$$\frac{\partial \mu_1(l)}{\partial l} = y_{1t} \mu_1(l) + (y_{1c} - y_{1t}) \mu_1(l) \mu_2(l). \quad (3.3a)$$

We could use a similar interpolation equation for  $\mu_h$  with  $y_{ht} = \frac{1}{2}(d + 2 - \eta_t)$  and  $y_{hc} = \frac{1}{2}(d + 2 - \eta_c)$ . However, we will neglect the difference between  $\eta_t$  and  $\eta_c$  and thus obtain

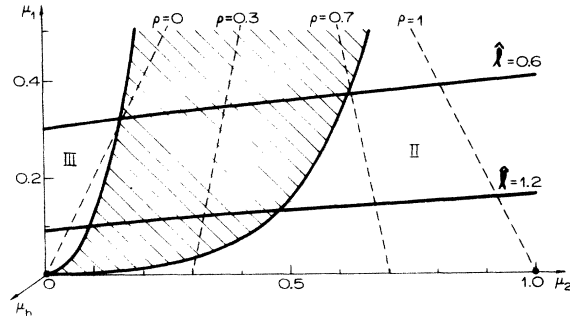


FIG. 1. Phase diagram in the  $(\mu_1, \mu_2, \mu_3)$  scaling-field space. The tricritical fixed point is located at  $(0, 0, 0)$  and the critical fixed point at  $(0, 1, 0)$ . The shaded area in the  $(\mu_1, \mu_2)$  plane denotes the crossover region. It separates the asymptotic tricritical region (III) from the asymptotic second-order critical region (II). The dashed lines are paths of  $\rho = \text{const}$ , which correspond to paths  $G = \text{const}$  in the phase diagram of Fig. 2. The lines  $\hat{l} = \text{const}$  will be defined in Sec. IV B.

$$\frac{\partial \mu_h(l)}{\partial l} = y_h \mu_h(l), \quad (3.3b)$$

with

$$y_h = \frac{1}{2}(d + 2 - \eta).$$

Finally, the operator  $Q_2$  conjugate to  $\mu_2$  is relevant for the tricritical point but irrelevant for the critical point. The simplest equation describing this behavior is

$$\frac{\partial \mu_2(l)}{\partial l} = y_{2t} \mu_2(l) [1 - \mu_2(l)]. \quad (3.3c)$$

The scaling indices of  $\mu_2$  (or  $Q_2$ ) are  $y_{2t}$  at the tricritical point and  $y_{2c} = -y_{2t}$  at the critical point. [Compare Eqs. (3.9) and (3.12).] Although one index is not necessarily the negative of the other, this is a good approximation in several cases where two fixed points as functions of a parameter intersect. For example, at dimensionality  $d = 4 - \epsilon$ , with  $\epsilon > 0$ , one obtains  $y_2 = \pm \epsilon + O(\epsilon^2)$  for the Gaussian tricritical fixed point and the non-Gaussian critical fixed point.<sup>7,25,26</sup> ( $y_2$  is identical with  $y_{20}$  and  $y_{2s}$  in the notation of Refs. 7 and 25.) This is related to the fact that  $\mu_2 = u$  (where  $u$  is the coefficient in Wilson's renormalization-group Hamiltonian) satisfies Eq. (3.3c) to leading order in  $\epsilon$  provided we scale according to Eq. (3.1).

Equations (3.3) constitute the basic equations of our model. Depending on the choice of the asymptotic scaling indices  $y_i$  these equations allow us to describe different physical situations. In Secs. V-VII we discuss numerically effective critical exponents for three particularly interesting three-dimensional models with crossover phenomena.

(i) *Tricritical model.* We study the tricritical model with molecular-field-like tricritical expo-

nents<sup>6,7</sup> and approximate critical-line exponents, starting from the set of scaling indices

$$\begin{aligned} y_{1t} &= 2, \quad y_{2t} = 1, \\ y_{1c} &\approx 1.5, \quad y_h \approx 2.5. \end{aligned} \quad (3.4)$$

We approximate  $\eta$  to be  $\eta = 0$ .

(ii) *Ashkin-Teller model*. We discuss the three-dimensional generalization of the Ashkin-Teller model,<sup>10</sup> which can be defined by two Ising spins  $S$  and  $T$  attached to each lattice site interacting via<sup>11</sup>

$$-H = K \sum_{\langle ij \rangle} (S_i S_j + T_i T_j + \bar{x} S_i S_j T_i T_j). \quad (3.5)$$

From high-temperature-series expansions one obtains for the uncoupled Ising models ( $\bar{x} = 0$ )  $y_1 = 1.6$  by using  $d/y_1 = 2 - \alpha$ , with  $\alpha = \frac{1}{8}$ . Therefore the interaction term  $\delta \epsilon_S \delta \epsilon_T$ , where  $\delta \epsilon_S = S_i S_j - \langle S_i S_j \rangle$ , scales like  $r^{-2x_1}$  (compare Ref. 27), with  $x_1 = d - y_1 = 1.4$ , which yields  $y_2 = d - 2x_1 = 0.2$ .<sup>28</sup> Hence the interaction term is a relevant operator, and the model is characterized by Ising-like tricritical exponents

$$y_{1t} = 1.6, \quad y_{2t} = 0.2. \quad (3.6a)$$

For  $y_{1c}$  and  $y_h$  we choose

$$y_{1c} \approx 2.2, \quad y_h \approx 2.5, \quad (3.6b)$$

where we use the approximation  $\eta = 0$ . The determination of  $y_{1c}$  is a subtle problem. Here we give only the argument for our choice and defer further discussion to Appendix A. We have estimated  $y_{1c}$ , using numerical data for the critical exponent  $\gamma$  for model (3.5) with  $\bar{x} = 1$ . High-temperature-series expansions yield  $\gamma = 0.91$ ,<sup>18</sup> which with  $\eta \approx 0$  leads to  $y_{1c} \approx 2/\gamma = 2.2$ .

(iii) *Fisher exponent renormalization*. We consider models with phase transitions subject to a constraint (such as decorated Ising models) which exhibit Fisher exponent renormalization.<sup>13</sup> If the system is governed by an index  $y_1 = d/(2 - \alpha) > \frac{1}{2}d$  (i. e.,  $\alpha > 0$ ), then the critical crossover phenomena due to Fisher renormalization can be described by Eqs. (3.3) with the asymptotic critical indices

$$y_{1t} = y_1, \quad y_{2t} = 2y_1 - d, \quad y_{1c} = d - y_1. \quad (3.7)$$

For decorated Ising models we take  $y_1 = 1.6$ , using the ideal three-dimensional Ising value  $\alpha = \frac{1}{8}$ .

In the present analysis we will accept the values (3.4), (3.6), and (3.7) for the asymptotic critical indices without further question. We note that the ratio  $y_{2t}/y_{1t} = \phi_t$  defines the crossover exponent introduced by the authors.<sup>14</sup> Therefore, the main difference between the models (i) and (ii) is in the size of the crossover exponent.

#### B. Thermodynamic quantities

Once we know the solutions of a given set of scaling-field equations and the value of a thermo-

dynamic quantity along a "noncritical boundary" we can calculate the thermodynamic quantity, including its scaling function, for the entire critical region.

The solutions of Eqs. (3.3a) and (3.3c) for  $\mu_i(l)$ , with  $i = 1, 2$ , are

$$\mu_1(l) = g_{1t}(l) [1 + g_{2t}(l)]^{(y_{1c} - y_{1t})/y_{2t}}, \quad (3.8a)$$

$$\mu_2(l) = g_{2t}(l) / [1 + g_{2t}(l)], \quad (3.8b)$$

with the *tricritical*  $g$  scaling fields

$$g_{1t}(l) = g_{1t} e^{y_{1t} l}, \quad g_{2t}(l) = g_{2t} e^{y_{2t} l}. \quad (3.9)$$

The solution of Eq. (3.3b) is

$$\mu_h(l) = h e^{y_h l}. \quad (3.10)$$

The solutions  $\mu_i(l)$  of Eqs. (3.3a) and (3.3c) can also be expressed in terms of scaling fields  $g_{ic}(l)$  relative to the critical fixed point,

$$\mu_1(l) = g_{1c}(l) [1 + g_{2c}(l)]^{(y_{1c} - y_{1t})/y_{2t}}, \quad (3.11a)$$

$$\mu_2(l) = 1 / [1 + g_{2c}(l)], \quad (3.11b)$$

with the *critical*  $g$  scaling fields given by

$$g_{1c}(l) = g_{1c} e^{y_{1c} l}, \quad g_{2c}(l) = g_{2c} e^{-y_{2t} l}. \quad (3.12)$$

The critical and tricritical  $g$  scaling fields are related,

$$g_{1c}(l) = g_{1t}(l) [g_{2t}(l)]^{(y_{1c} - y_{1t})/y_{2t}}, \quad (3.13a)$$

$$g_{2c}(l) = 1/g_{2t}(l). \quad (3.13b)$$

Equation (3.8) in the limit  $l = 0$  allows the parameter  $g_{it}$  to be expressed in terms of the initial scaling fields  $\mu_i$ ,

$$\begin{aligned} g_{1t} &= \mu_1 (1 - \mu_2)^{(y_{1c} - y_{1t})/y_{2t}}, \\ g_{2t} &= \mu_2 / (1 - \mu_2). \end{aligned} \quad (3.14)$$

Similar relations for  $g_{ic}$  follow from Eq. (3.11).

The two representations for the solutions of the equation of motion (3.3) in Eqs. (3.8) and (3.9), and Eqs. (3.11) and (3.12) reflect the symmetry between the tricritical fixed point and the critical fixed point in our model. Equations (3.3) and (3.8)–(3.13) are invariant under the transformation

$$\begin{aligned} &(\mu_1, \mu_2, g_{1t}, g_{2t}, g_{1c}, g_{2c}, y_{1t}, y_{1c}, y_{2t}) \\ &\rightarrow (\mu_1, 1 - \mu_2, g_{1c}, g_{2c}, g_{1t}, g_{2t}, y_{1c}, y_{1t}, -y_{2t}). \end{aligned} \quad (3.15)$$

The two fixed points are only distinguished by  $y_{2t} > 0$  and  $y_{2c} = -y_{2t} < 0$ . The scaling field  $g_{2t}(l)$  is relevant at the tricritical fixed point and the scaling field  $g_{2c}(l)$  is irrelevant at the critical fixed point.

The initial scaling fields  $\mu_i$  are functions of two experimental fields, which we take to be the temperature  $T$  and a nonordering field  $G$ .<sup>17</sup> (The experimental field  $G$  is irrelevant along the critical

line but relevant at the tricritical point.) Similarly to Eqs. (3.8)–(3.11) of Ref. 4 we expand in terms of the eigenoperators  $Q_i$  [compare Eq. (2.3)] both the fixed point Hamiltonian,

$$H^* = -\sum_i h_i^* Q_i, \quad (3.16)$$

and the Hamiltonian  $\mathcal{H}$  of the system,

$$\begin{aligned} \mathcal{H}(G) &= \mathcal{H}(0) + GV \\ &= \sum_i (h_i^0 + Gh_i^1) Q_i. \end{aligned} \quad (3.17)$$

By comparison with expansion (2.3) for the reduced initial Hamiltonian  $H_0$ , we obtain for the initial scaling fields  $\mu_i$ ,

$$\mu_i = h_i^* - \beta(h_i^0 + Gh_i^1), \quad (3.18)$$

with  $\beta = 1/k_B T$ . (We absorb in the coefficient  $h_i^*$  contributions from the phase-space weight factor.) Therefore, the specification of the initial scaling fields  $\mu_i$  amounts to the specification of all interaction parameters and of the values of all experimental fields. The condition  $\mu_i = 0$  yields for the critical temperature

$$k_B T_c(G) = (h_1^0 + Gh_1^1)/h_1^*. \quad (3.19)$$

We are free to choose the scale for  $\mu_1$  by  $h_1^* = 1$ , which yields

$$\mu_1 = 1 - \beta/\beta_c(G). \quad (3.20)$$

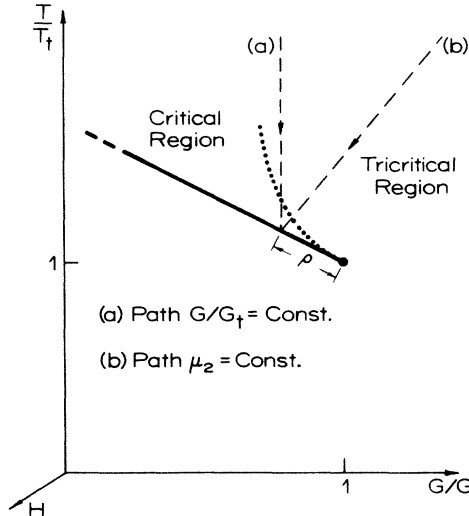


FIG. 2. Schematic phase diagram in the experimental  $(T, G, H)$  field space. The phase diagram consists of a linear critical line [in the  $(T, G)$  plane] that terminates in a tricritical point. Two kinds of paths of approach to criticality are shown: (a) lines of  $G/G_t = \text{const.}$  and (b) lines of  $\mu_2 = \text{const.}$  The quantity  $\rho(G)$  measures the departure of a point on the critical line from the tricritical point. The dotted line denotes the approximate center of the crossover region separating the tricritical region and the critical region.

For the scaling field  $\mu_2$  we find

$$\mu_2 = \rho(G) + r(G) \mu_1, \quad (3.21)$$

with

$$\rho(G) = h_2^* - r(G), \quad (3.22)$$

$$r(G) = (h_2^0 + Gh_2^1)/(h_1^0 + Gh_1^1). \quad (3.23)$$

The tricritical field  $G = G_t$  is determined by

$$\rho(G_t) = 0. \quad (3.24)$$

Therefore,  $\rho$  is a measure for the departure of  $G$  from its tricritical value  $G_t$ . Hence the phase diagram of the model in the  $(T, G)$  plane exhibits a critical line which varies linearly with the experimental field  $G$  and terminates in a tricritical point, as shown in Fig. 2.

The thermodynamic potential  $F$  of the system is a homogeneous function in the  $g$  scaling fields or a *generalized* homogeneous function in the  $\mu$  scaling fields [compare Eq. (2.4)],

$$F(\mu_1, \mu_2, \mu_h) = e^{-dI} F(\mu_1(I), \mu_2(I), \mu_h(I)). \quad (3.25)$$

For simplicity we write Eq. (3.25) and similar relations in the form  $F = e^{-dI} F(I)$ . Equation (3.25) implies for the ordering density (*with*  $\eta = 0$ )

$$\begin{aligned} m &= \frac{\partial F}{\partial h} = e^{(1-d/2)I} \frac{\partial F(I)}{\partial \mu_h(I)} \\ &= e^{(1-d/2)I} m(I), \end{aligned} \quad (3.26)$$

and for the susceptibility

$$\chi = \frac{\partial^2 F}{\partial h^2} = e^{2I} \chi(I). \quad (3.27)$$

(The susceptibility  $\chi$  contains a factor  $1/\beta$ ; hence, in the limit  $\beta \rightarrow 0$  the Curie law  $\chi \propto 1/T$  follows.)

Equation (3.27) allows the evaluation of the susceptibility  $\chi$  provided the quantity is known along a "boundary." We assume that the system is outside its critical region when the boundary

$$\mu_1(\hat{l}) = 1 \quad (3.28)$$

is reached, and we denote  $\mu_2(l)$  along this boundary by  $\hat{\mu}_2$ ,

$$\mu_2(\hat{l}) = \hat{\mu}_2. \quad (3.29)$$

Then we obtain from Eq. (3.27) for the susceptibility

$$\chi(\mu_1, \mu_2, 0) = e^{2\hat{l}} \bar{\chi}(\hat{\mu}_2), \quad (3.30)$$

with

$$\bar{\chi}(\hat{\mu}_2) = \chi(1, \hat{\mu}_2, 0). \quad (3.31)$$

Equation (3.30) yields the susceptibility  $\chi$  in the critical region as a function of the two coordinates  $\hat{l}$  and  $\hat{\mu}_2$ , and in terms of the susceptibility  $\bar{\chi}(\hat{\mu}_2)$  along a boundary *outside* the critical region.<sup>29</sup>

Since  $\bar{\chi}(\hat{\mu}_2)$  describes the susceptibility outside the critical region we can assume that it is a smooth function of  $\hat{\mu}_2$ . Therefore, the critical properties of  $\chi$  are contained in the quantity  $\hat{l}$ . Both  $\hat{l}$  and  $\hat{\mu}_2$  are functions of the two experimental fields  $T$  and  $G$  via the initial scaling fields  $\mu_1$  and  $\mu_2$ . The result (3.30) for the susceptibility does not depend on the choice (3.3) of model equations for the scaling fields.

Thermodynamic quantities other than the susceptibility can be analogously determined.

### C. Discussion of the model

Before we consider the scaling properties of the susceptibility (3.30) in detail it is appropriate to discuss the main effects of our approximations. First, we consider only three scaling fields ( $\mu_1, \mu_2, \mu_h$ ) although other fields may contribute corrections.<sup>4,7</sup> In particular, we have neglected the marginal scaling field  $\mu_3$  in the tricritical model (i) which would lead to logarithmic corrections.<sup>7</sup> Moreover, the irrelevant fields may contribute considerably at high temperatures, i. e.,  $\beta \ll \beta_c$ . [Within our theory improved results for  $\chi$  near criticality can be obtained by matching  $\chi$  and  $\bar{\chi}(\hat{\mu}_2)$  along boundaries  $\mu_1(\hat{l}) = 0.1$  or  $0.01$  instead of along  $\mu_1(\hat{l}) = 1$ .] Second, owing to the special choice of the Eqs. (3.3) the critical temperature varies linearly with  $\mu_2$ . In Appendix B we will briefly discuss a more general model, for which we find  $[T_c(\mu_2) - T_c(0)]_{\text{sing}} \propto \mu_2^{1/\phi_t}$ , as is expected.<sup>6,17</sup> Finally, the choice of the scale for  $\mu_2$  by definition (3.1) has the effect that we obtain a "fixed line" for  $y_{2t} = 0$  but not the logarithmic singularities discussed in Ref. 7.

## IV. SCALING PROPERTIES OF THE SUSCEPTIBILITY

The model (3.3) implies the scaling properties of all thermodynamic quantities. As an example we discuss the scaling behavior of the susceptibility defined by Eqs. (3.30) and (3.31).

### A. Determination of scaling functions

The condition  $\mu_1(\hat{l}) = 1$  in Eq. (3.28) can be cast in the form

$$z = (1 + cz)^\sigma. \quad (4.1)$$

We denote the solution of this equation by

$$\begin{aligned} z &= f(\sigma, c) \\ &= 1 + \sigma c + \frac{1}{2}\sigma(3\sigma - 1)c^2 + O(c^3). \end{aligned} \quad (4.2)$$

Starting from Eq. (3.8a) or (3.11a), we find for the quantities in Eq. (4.1)

$$z_c = \mu_1^{-y_{2t}/y_{1t}} \mu_2^{-\sigma_c} e^{-y_{2t}\hat{l}}, \quad (4.3a)$$

$$\sigma_c = (y_{1c} - y_{1t})/y_{1c}, \quad (4.3b)$$

$$c_c = C^{y_{2t}/y_{1c}}, \quad (4.3c)$$

or

$$z_t = \mu_1^{y_{2t}/y_{1t}} (1 - \mu_2)^{-\sigma_t} e^{y_{2t}\hat{l}}, \quad (4.4a)$$

$$\sigma_t = (y_{1t} - y_{1c})/y_{1t}, \quad (4.4b)$$

$$c_t = C^{-y_{2t}/y_{1t}}, \quad (4.4c)$$

with

$$C = \mu_1(1 - \mu_2)^{y_{1c}/y_{2t}} \mu_2^{-y_{1t}/y_{2t}}. \quad (4.5)$$

The exponents  $\sigma_t$  and  $\sigma_c$  are related,  $\sigma_t/\sigma_c = -y_{1c}/y_{1t}$ . We can determine  $\hat{l}$  from Eqs. (4.1)–(4.4),

$$e^{-y_{2t}\hat{l}} = \mu_1^{y_{2t}/y_{1c}} \mu_2^{\sigma_c} f(\sigma_c, c_c), \quad (4.6)$$

$$e^{y_{2t}\hat{l}} = \mu_1^{-y_{2t}/y_{1t}} (1 - \mu_2)^{\sigma_t} f(\sigma_t, c_t). \quad (4.7)$$

Then Eq. (3.30) implies for the susceptibility

$$\chi(\mu_1, \mu_2) = \mu_1^{-2/y_{1c}} \mu_2^{-2\sigma_c/y_{2t}} v_c(c_c), \quad (4.8a)$$

with

$$\begin{aligned} v_c(c_c) &= \bar{\chi}(\hat{\mu}_2(c_c^{y_{1c}/y_{2t}})) \\ &\times [f(\sigma_c, c_c)]^{-2/y_{2t}}. \end{aligned} \quad (4.8b)$$

and

$$\chi(\mu_1, \mu_2) = \mu_1^{-2/y_{1t}} (1 - \mu_2)^{2\sigma_t/y_{2t}} v_t(c_t), \quad (4.9a)$$

with

$$\begin{aligned} v_t(c_t) &= \bar{\chi}(\hat{\mu}_2(c_t^{-y_{1t}/y_{2t}})) \\ &\times [f(\sigma_t, c_t)]^{2/y_{2t}}. \end{aligned} \quad (4.9b)$$

The relations in the pairs of equations (4.3) and (4.4), (4.6) and (4.7), and (4.8) and (4.9) are equivalent [in agreement with Eq. (3.15)]. Equations (4.8) and (4.9) constitute the main result of this section; they contain the general scaling properties of the susceptibility  $\chi$  with the *scaling functions*  $v$  determined by Eqs. (4.8b) and 4.9b).<sup>30</sup>

The variable  $C$  in Eq. (4.5) plays the role of a reduced relative temperature.<sup>31</sup> The scale factor  $(1 - \mu_2)^{y_{1c}/y_{2t}} \mu_2^{-y_{1t}/y_{2t}}$  diverges at the tricritical fixed point and vanishes at the critical fixed point. This indicates that the asymptotic (or ideal) critical behavior holds in a large temperature region around the critical fixed point but shrinks to zero at the tricritical fixed point. Scaling variables such as  $C$  are singled out in that they are *constants of the motion* (invariants) of the renormalization-group procedure. One easily finds from Eqs. (3.3) that  $dC(l)/dl = 0$ . Therefore  $C$  is a function of  $\hat{\mu}_2$  only; Eq. (4.5) yields for  $l - \hat{l}$

$$C = (1 - \hat{\mu}_2)^{y_{1c}/y_{2t}} \hat{\mu}_2^{-y_{1t}/y_{2t}}, \quad (4.10)$$

which defines a function  $\hat{\mu}_2(C)$ .

If we express the susceptibility in Eqs. (4.8) and (4.9) in terms of the  $g$  scaling fields we discover that it has exactly the scaling form that had been postulated in our scaling theories for crossover phenomena.<sup>14,17</sup> In particular,  $C$  plays the role of

the reduced scaling variable of these theories,

$$C = g_{1t} g_{2t}^{-y_{1t}/y_{2t}} \text{ or } C = g_{1c} g_{2c}^{y_{1c}/y_{2c}}. \quad (4.11)$$

The results can be written in a more familiar notation by introducing the Greek-alphabet exponents

$$\gamma_t = 2/y_{1t}, \quad \phi_t = y_{2t}/y_{1t}, \quad (4.12a)$$

$$\gamma_c = 2/y_{1c}, \quad \phi_c = -y_{2t}/y_{1c}. \quad (4.12b)$$

Finally we discuss the scaling behavior of the susceptibility in various asymptotic regions.

(i) *Scaling near the tricritical fixed point.* In the whole region around the tricritical fixed point,  $\mu_2 \ll 1$ .<sup>32</sup> Hence we obtain from Eq. (4.9a)

$$\chi(\mu_1, \mu_2) = \mu_1^{-2/y_{1t}} v_t(\mu_2 \mu_1^{-y_{2t}/y_{1t}}). \quad (4.13)$$

This and the following results exhibit the structure expected from crossover scaling. The area around the tricritical point contains the asymptotic tricritical region  $c_t \ll 1$  and a part of the asymptotic critical region  $c_c \ll 1$ , which are separated by a crossover region, as shown in Fig. 1.

(ii) *Scaling in the asymptotic tricritical region.* In the asymptotic tricritical region,  $c_t \ll 1$ ,<sup>32</sup> we may expand  $\hat{\mu}_2$  and  $v_t$  into powers of  $c_t$ . From Eq. (4.4c) we obtain

$$\hat{\mu}_2 = c_t(1 - \hat{\mu}_2)^{y_{1c}/y_{1t}} = c_t + O(c_t^2), \quad (4.14)$$

and from Eqs. (4.9b) and (4.2)

$$v_t(c_t) = \bar{\chi}(0) \left[ 1 + \left( \frac{2\sigma_t}{y_{2t}} + \frac{\partial \ln \bar{\chi}}{\partial \hat{\mu}_2} \Big|_{\hat{\mu}_2=0} \right) c_t + O(c_t^2) \right]. \quad (4.15)$$

Hence, in addition to the power-law behavior  $\chi = \mu_1^{-\gamma_t} \bar{\chi}(0)$  one obtains a correction proportional to  $\mu_1^{-\sigma_t}$  with an amplitude proportional to  $\mu_2$ .

(iii) *Scaling in the critical region.* In the critical region,  $c_c \ll 1$ ,<sup>32</sup> we start from Eq. (4.8a) and expand into powers of  $c_c$ . From Eq. (4.3c) we obtain

$$\begin{aligned} \hat{\mu}_2 &= 1 - c_c \hat{\mu}_2^{y_{1t}/y_{1c}} \\ &= 1 - c_c + O(c_c^2), \end{aligned} \quad (4.16)$$

which, when substituted into Eqs. (4.8), yields

$$\begin{aligned} \chi(\mu_1, \mu_2) &= \mu_1^{-2/y_{1c}} \mu_2^{-2\sigma_c/y_{2t}} \bar{\chi}(1) \\ &\times \left[ 1 - \left( \frac{2\sigma_c}{y_{2t}} + \frac{\partial \ln \bar{\chi}}{\partial \hat{\mu}_2} \Big|_{\hat{\mu}_2=1} \right) c_c + O(c_c^2) \right]. \end{aligned} \quad (4.17)$$

The leading term in this expansion is the "double-scaling" term, which is characterized by the critical-line exponent  $\gamma_c$  and the amplitude exponent  $2\sigma_c/y_{2t} = (\gamma_t - \gamma_c)/\phi_t$ . The first correction to the pure power-law behavior is a factor of  $c_c$  smaller than the leading term. Since as a function of  $\mu_1$

Eq. (4.3c) yields  $c_c \propto \mu_1^{y_{2t}/y_{1c}}$ , this correction is in agreement with the prediction of Eq. (1.1) of Ref. 4. (Note that the latter equation is written in terms of  $g_c$  scaling fields.) The correction term vanishes (since  $c_c$  vanishes) for the critical path  $\mu_2 = 1$ . Therefore, one finds only for  $\mu_2 = 1$  a pure power-law behavior. This value of  $\mu_2$  corresponds to Wilson's choice<sup>33</sup> of the coefficient  $u_0(\epsilon)$  to eliminate the slow transient.

The complete scaling behavior of the susceptibility in the whole critical region (including the crossover regions) is contained in Eqs. (4.8) and (4.9) and will be numerically discussed in Sec. V.

### B. Flow diagram in the scaling-field space

Here we discuss briefly the topology of crossover phenomena in the scaling-field space, and the physical meaning of the coordinates  $\hat{l}(\mu_1, \mu_2)$  and  $\hat{\mu}_2(\mu_1, \mu_2)$  in Eq. (3.30).

The scale parameter  $e^{2\hat{l}}$  connects the values of the susceptibility  $\chi$  in the two states  $(\mu_1, \mu_2)$  and  $(1, \hat{\mu}_2)$ . Therefore, lines of  $\hat{l}(\mu_1, \mu_2) = \text{const}$  define "surfaces" in the scaling-field space [i. e., lines in the  $(\mu_1, \mu_2)$  plane] of  $\chi/\bar{\chi} = \text{const}$ . Two such lines are shown in Fig. 1. The "critical surface" is defined by  $\hat{l} = \infty$  or  $\chi = \infty$ . It is the line connecting the tricritical and the critical fixed point. Renormalization-group equations such as (3.3) determine how as a function of  $l$  the initial state  $(\mu_1, \mu_2)$  changes continuously into  $(\mu_1(l), \mu_2(l))$ . The lines connecting these states define "trajectories" in the scaling-field space that cross all surfaces of constant  $\chi(l) < \chi(0)$ . On each trajectory the susceptibility scales according to Eq. (3.27). The trajectories can be defined by  $\hat{\mu}_2(\mu_1, \mu_2) = \hat{\mu}_2(1, \hat{\mu}_2) = \text{const}$ . ( $\hat{\mu}_2$  is a number between 0 and 1 for  $\mu_1$  and  $\mu_2$  both in the interval  $[0, 1]$ .) In the following we will refer to the set of surfaces and trajectories in the scaling-field space as the *flow diagram* of the transition.

Equations (3.8) or (3.11) determine the flow diagram for our model. Eqs. (3.11) imply that all trajectories starting on the critical surface approach the critical fixed point, and that a single trajectory ( $\hat{\mu}_2 = 1$ ) leaves the critical fixed point. In contrast, Eq. (3.8) implies that no trajectory approaches the tricritical fixed point, whereas infinitely many (with  $0 \leq \hat{\mu}_2 < 1$ ) leave it. (Two such trajectories are the lines that bound the crossover region in Fig. 1.) These different patterns of flow in the neighborhoods of the critical fixed point and the tricritical fixed point characterize the topological differences between these fixed points.<sup>34</sup>

Equation (4.10) implies that a trajectory  $\hat{\mu}_2$  defines also a scaling path  $C = \text{const}$  in the sense of the conventional theory. (Note that the trajectories  $\hat{\mu}_2 = 0$  and  $\hat{\mu}_2 = 1$  are singled out in that pure power laws hold along these paths of approach to

criticality.<sup>32)</sup> This result suggests that on each trajectory the *degree* of singularity of  $\chi$  is constant, although the absolute value of  $\chi$  decreases. In fact, we will find in Eq. (5.12) that along each trajectory  $\hat{\mu}_2$  the logarithmic derivative  $\partial \ln \chi / \partial \ln \mu_1$  is constant. Its value measures the relative influence of the critical fixed point and the tricritical fixed point on the critical behavior along the *whole* trajectory.<sup>32</sup> This in turn allows the critical region to be divided into areas of effectively critical and tricritical behavior which, as shown in Fig. 1, are separated by a possibly broad crossover region.

### V. EFFECTIVE CRITICAL EXPONENTS

If the location of the asymptotic critical region(s) is not known in a laboratory experiment or in a computer experiment, then its analysis in terms of asymptotic critical exponents may become difficult or meaningless. It is then preferable to introduce effectively field-dependent critical exponents at each point of the field space. This concept of effective critical and tricritical exponents is introduced in the following paragraphs.<sup>35</sup> As an example we discuss again the critical and tricritical behavior of the susceptibility  $\chi$ .

#### A. Effective exponents and size of crossover regions

We define an effective critical exponent  $\gamma_{\text{eff}}$  for the susceptibility  $\chi$  at each point in the  $(\mu_1, \mu_2)$  scaling-field space by the logarithmic derivative

$$\gamma_{\text{eff}}(\mu_1, \mu_2) = - \frac{d \ln \chi(\mu_1, \mu_2)}{d \ln \mu_1} . \quad (5.1)$$

Effective exponents for other thermodynamic quantities are similarly defined. The effective exponent  $\gamma_{\text{eff}}$  provides a local measure for the degree of singularity of  $\chi$  at  $(\mu_1, \mu_2)$ . When the point  $(\mu_1, \mu_2)$  approaches a critical (or tricritical) point then  $\gamma_{\text{eff}}$  becomes identical with the corresponding asymptotic critical exponent  $\gamma$ . However, the definition (5.1) avoids the hidden question whether one is close enough to criticality to be able to see the true asymptotic value of the exponent. Moreover, since the effective exponent is locally defined it reflects very sensitively crossover phenomena, i. e., a different critical behavior in different areas of the critical region. From that viewpoint the concept of effective exponents is particularly useful for the discussion of systems with competing phase transitions. In the following we calculate the effective exponent  $\gamma_{\text{eff}}$  for the model defined by the scaling-field equations (3.3).

Starting from Eq. (4.8) for the susceptibility  $\chi$ , we obtain for the effective exponent along a path of constant  $\mu_2$

$$\dot{\gamma}_{\text{eff}}(\mu_1, \mu_2) = \frac{2}{\gamma_{1c}} \left( 1 + \frac{\partial \ln f(\sigma_c, c_c)}{\partial \ln c_c} \right) - \frac{d \ln \bar{\chi}}{d \ln C} . \quad (5.2)$$

The fluxion dot on  $\dot{\gamma}_{\text{eff}}$  denotes that the exponent is taken along a path  $\mu_2 = \text{const.}$  (Whereas asymptotic exponents are path independent, effective exponents do depend on the path along which criticality is approached.) The result (5.2) for the effective exponent depends on the two fields  $\mu_1$  and  $\mu_2$  only through the scaling variable  $C$  or, because of the relation (4.10), through  $\hat{\mu}_2$ ,

$$\begin{aligned} \dot{\gamma}_{\text{eff}} &= \dot{\gamma}_{\text{eff}}(C) \\ &\equiv \dot{\gamma}_{\text{eff}}(\mu_1(1 - \mu_2)^{\gamma_{1c}/\gamma_{2t}} \mu_2^{-\gamma_{1t}/\gamma_{2t}}) . \end{aligned} \quad (5.3)$$

We introduce an effective scaling index  $y_{1,\text{eff}}(\hat{\mu}_2)$ , which we define by

$$y_{1,\text{eff}} = \gamma_{1,c} / \left( 1 + \frac{\partial \ln f}{\partial \ln c_c} \right) . \quad (5.4)$$

[In Eqs. (5.4)–(5.7)  $f$  means  $f(\sigma_c, c_c)$ .] Using the definition (4.2) for  $f$ , i. e.,  $f = (1 + cf)^\sigma$ , we obtain

$$y_{1,\text{eff}} = \gamma_{1c} \left( 1 - \frac{\sigma_c c_c f}{1 + c_c f} \right) , \quad (5.5)$$

from which we deduce

$$y_{1c} - y_{1,\text{eff}} = (y_{1c} - y_{1t}) \frac{c_c f}{1 + c_c f} , \quad (5.6a)$$

$$y_{1,\text{eff}} - y_{1t} = (y_{1c} - y_{1t}) \frac{1}{1 + c_c f} . \quad (5.6b)$$

The relative deviations of  $y_{1,\text{eff}}$  from the asymptotic scaling indices  $y$  therefore satisfy

$$\begin{aligned} &\left( \frac{y_{1c} - y_{1,\text{eff}}}{y_{1c} - y_{1t}} \right)^{\gamma_{1c}/\gamma_{2t}} \left( \frac{y_{1,\text{eff}} - y_{1t}}{y_{1c} - y_{1t}} \right)^{-\gamma_{1t}/\gamma_{2t}} \\ &= (c_c f)^{\gamma_{1c}/\gamma_{2t}} (1 + c_c f)^{-(y_{1t} - y_{1c})/\gamma_{2t}} \\ &= c_c^{\gamma_{1c}/\gamma_{2t}} \\ &= C . \end{aligned} \quad (5.7)$$

By comparing this result with Eq. (4.10) we find

$$\frac{y_{1,\text{eff}} - y_{1t}}{y_{1c} - y_{1t}} = \hat{\mu}_2 , \quad (5.8)$$

from which we obtain

$$y_{1,\text{eff}}(\hat{\mu}_2) = y_{1t} + \hat{\mu}_2 (y_{1c} - y_{1t}) . \quad (5.9)$$

Finally we evaluate

$$- \frac{d \ln \bar{\chi}}{d \ln C} = - \frac{d \ln \bar{\chi}}{d \hat{\mu}_2} / \frac{d \ln C}{d \hat{\mu}_2} . \quad (5.10)$$

Equation (4.10) yields

$$\frac{d \ln C}{d \hat{\mu}_2} = - \frac{y_{1,\text{eff}}(\hat{\mu}_2)}{\gamma_{2t} \hat{\mu}_2 (1 - \hat{\mu}_2)} . \quad (5.11)$$

Substituting the results (5.4), (5.9)–(5.11) into Eq. (5.2), we obtain for the effective exponent  $\dot{\gamma}_{\text{eff}}$  as a function of  $\hat{\mu}_2$  (or  $C$ )

$$\begin{aligned} \dot{\gamma}_{\text{eff}}(\mu_1, \mu_2) &= \left[ 2 + \gamma_{2t} \hat{\mu}_2 (1 - \hat{\mu}_2) \frac{d \ln \bar{\chi}(\hat{\mu}_2)}{d \hat{\mu}_2} \right] / y_{1, \text{eff}}(\hat{\mu}_2). \end{aligned} \quad (5.12)$$

The effective exponent  $\dot{\gamma}_{\text{eff}}$  is *constant* along the trajectories  $\hat{\mu}_2$ . It approaches the asymptotic exponents  $\gamma_c$  and  $\gamma_t$  for  $\hat{\mu}_2 \rightarrow 0$  and  $\hat{\mu}_2 \rightarrow 1$ , respectively. [The derivative of the smooth function  $\bar{\chi}$  does not affect the asymptotic exponents because of the factor  $\hat{\mu}_2(1 - \hat{\mu}_2)$ .] The onset of the departure of  $\dot{\gamma}_{\text{eff}}$  from  $\gamma_t$  and  $\gamma_c$  can be obtained from Eq. (5.12) by using the expansions (4.14) and (4.16). In the tricritical region we find

$$\dot{\gamma}_{\text{eff}} = \gamma_t \left[ 1 + \left( \sigma_t + \frac{1}{2} \gamma_{2t} \frac{d \ln \bar{\chi}}{d \hat{\mu}_2} \Big|_{\hat{\mu}_2=0} \right) c_t + O(c_t^2) \right], \quad (5.13a)$$

and in the critical region we obtain

$$\dot{\gamma}_{\text{eff}} = \gamma_c \left[ 1 + \left( \sigma_c + \frac{1}{2} \gamma_{2t} \frac{d \ln \bar{\chi}}{d \hat{\mu}_2} \Big|_{\hat{\mu}_2=1} \right) c_c + O(c_c^2) \right]. \quad (5.13b)$$

If the derivative  $d \ln \bar{\chi} / d \hat{\mu}_2$  in Eq. (5.12) and the effect of  $d \mu_2 / d \mu_1 \neq 0$  [compare Eq. (5.21) below] are negligible then we can easily *estimate* the size of the crossover region for the susceptibility  $\chi$ . We define the crossover region as the area of the  $(\mu_1, \mu_2)$  space in which the effective exponent  $\gamma_{1, \text{eff}}(\hat{\mu}_2)$  deviates by more than a fraction  $p$  (with  $0 < p < 1$ ) of the difference  $|y_{1c} - y_{1t}|$  from the asymptotic value  $y_{1c}$  or  $y_{1t}$ . [More precisely, we can define the crossover region in terms of deviations of  $\gamma_{\text{eff}}$  in Eq. (5.21) from  $\gamma_c$  and  $\gamma_t$ .] The size of ordinary critical regions can be defined similarly. According to our definition the  $p$  crossover region  $(\bar{\mu}_{1c}(p), \bar{\mu}_{1t}(p))$  is determined by

$$\hat{\mu}_2(\bar{\mu}_{1t}(p)) = p, \quad (5.14a)$$

$$\hat{\mu}_2(\bar{\mu}_{1c}(p)) = 1 - p. \quad (5.14b)$$

Using Eqs. (4.5) and (4.10) we can calculate the  $\bar{\mu}_{1t, c}$

$$\begin{aligned} \bar{\mu}_{1t}(p) &= \bar{\mu}_{1c}(1 - p) \\ &= (1 - p)^{y_{1c}/y_{2t}} p^{-y_{1t}/y_{2t}} \\ &\quad \times (1 - \mu_2)^{-y_{1c}/y_{2t}} \mu_2^{y_{1t}/y_{2t}}. \end{aligned} \quad (5.15)$$

Equations (5.15) allow us to estimate the size of the second-order critical region  $\bar{\mu}_{1c}(p)$  close to the critical line once the metric in the field space is known [compare Eqs. (3.20) and (3.21)]. The *width* of the  $p$  crossover region, which separates the tricritical region from the critical-line region, can be characterized by the ratio

$$W_{\text{CR}}(p) = \frac{\bar{\mu}_{1t}(p)}{\bar{\mu}_{1c}(p)}$$

$$= \left( \frac{1 - p}{p} \right)^{(y_{1c} + y_{1t})/y_{2t}}. \quad (5.16)$$

This equation contains *only* the asymptotic scaling indices  $y$ . The most interesting feature of the result is that the width of the crossover region  $W_{\text{CR}}$  increases strongly with decreasing  $y_{2t}$ ; i. e.,  $W_{\text{CR}}$  is larger the smaller the crossover exponent  $\phi_t$ . For the 25% crossover region we obtain as a rule of thumb (by approximating  $y_{1t} \approx y_{1c}$  and  $9 \approx 10$ )

$$W_{\text{CR}}(0.25) \approx 10^{1/\phi_t}. \quad (5.17)$$

Therefore, the 25% crossover region has approximately a width of  $1/\phi_t$  decades. (The 10% crossover region extends over twice as many decades and the 3% crossover region has three times as many decades.) These results hold for the susceptibility  $\chi$  only. For other thermodynamic quantities the critical indices in Eq. (5.16), apart from the characteristic dependence on the crossover exponent, are different.

So far we have only considered the effective exponent along a path  $\mu_2 = \text{const}$ . To evaluate the effective exponent  $\gamma_{\text{eff}}$  as a function of the experimental fields  $T$  and  $G$  we have to take into consideration that  $\mu_2$  is a function of  $\mu_1$ . We then obtain for the effective exponent (5.1)

$$\gamma_{\text{eff}} = \dot{\gamma}_{\text{eff}} - \mu_1 \frac{d \mu_2}{d \mu_1} \frac{\partial \ln \chi}{\partial \mu_2}. \quad (5.18)$$

From Eq. (4.8) we find

$$-\frac{\partial \ln \chi}{\partial \mu_2} = \frac{2\sigma_c}{y_{2t}\mu_2} + \left( \frac{2}{y_{1c}} \frac{\partial \ln f(\sigma_c, c_c)}{\partial \ln c_c} - \frac{d \ln \bar{\chi}}{d \ln C} \right) \frac{\partial \ln C}{\partial \mu_2}. \quad (5.19)$$

By using Eq. (5.2) the expression in large parentheses in Eq. (5.19) can be cast in the form  $(\dot{\gamma}_{\text{eff}} - 2/y_{1c})$ . With

$$\frac{\partial \ln C}{\partial \mu_2} = -\frac{y_{1t}}{y_{2t}\mu_2} - \frac{y_{1c}}{y_{2t}(1 - \mu_2)} \quad (5.20)$$

and the exponents (4.12) we obtain finally

$$\begin{aligned} \gamma_{\text{eff}} &= \dot{\gamma}_{\text{eff}} + \mu_1 \frac{d \mu_2}{d \mu_1} \left( \frac{1}{\mu_2} \frac{\gamma_t - \dot{\gamma}_{\text{eff}}}{\phi_t} \right. \\ &\quad \left. + \frac{1}{1 - \mu_2} \frac{\gamma_c - \dot{\gamma}_{\text{eff}}}{|\phi_c|} \right). \end{aligned} \quad (5.21)$$

The denominators  $\mu_2$  and  $(1 - \mu_2)$  in this equation do not lead to divergencies provided  $y_{2t} < y_{1t}$ . This result follows with the help of the asymptotic expressions (5.13) for  $\dot{\gamma}_{\text{eff}}$ . However, if  $d \mu_2 / d \mu_1$  becomes large then  $\gamma_{\text{eff}}$  can deviate strongly from  $\dot{\gamma}_{\text{eff}}$ . Equations (5.12) and (5.21) are the main results of this section.

#### B. Effects of almost marginal scaling fields

Here we study the case of a very small scaling index  $y_{2t}$ , i. e., a situation in which the scaling

fields  $g_{2c}$  and  $g_{2t}$  are almost marginal.

For  $y_{2t} = 0$  the Eqs. (3.3) yield  $\mu_2(l) = \text{const}$ , and the susceptibility becomes

$$\chi(\mu_1, \mu_2) = \bar{\chi}(\mu_2) \mu_1^{\gamma(\mu_2)}, \quad (5.22)$$

with

$$\gamma(\mu_2) = 2/y_{1,\text{eff}}(\mu_2). \quad (5.23)$$

Because of the ansatz (3.3c) we obtain a line of fixed points. In general, we expect for the case  $y_{2t} = 0$  an equation of the form  $\partial \mu_2 / \partial l = a \mu_2^2 + \dots$ , which leads to logarithmic corrections.<sup>7</sup>

In the following we choose  $y_{2t} \ll 1$ . We then expect only for very small  $\mu_1$  deviations from the effective exponent  $\gamma(\mu_2)$  in Eq. (5.23). From Eqs. (4.5) and (4.10) we obtain

$$\begin{aligned} \hat{\mu}_2 &= \mu_2 + y_{2t} \mu_2 (1 - \mu_2) \\ &\quad \times (\ln(1/\mu_1)) / y_{1,\text{eff}}(\mu_2) + O(y_{2t}^2) \end{aligned} \quad (5.24)$$

in the region

$$\mu_1 \gg \exp[-y_{1,\text{eff}}(\mu_2)/(1 - \mu_2)y_{2t}], \quad (5.25)$$

when  $\mu_2 \neq 0, 1$ . Substituting this result into Eq. (5.12) yields the effective exponent

$$\begin{aligned} \dot{\gamma}_{\text{eff}}(\mu_1, \mu_2) &= \frac{2}{y_{1,\text{eff}}(\mu_2)} \left\{ 1 + y_{2t} \mu_2 (1 - \mu_2) \right. \\ &\quad \times \left[ (y_{1t} - y_{1c}) (\ln(1/\mu_1)) / y_{1,\text{eff}}(\mu_2) \right. \\ &\quad \left. \left. + \frac{1}{2} \frac{d \ln \bar{\chi}}{d \hat{\mu}_2} \Big|_{\hat{\mu}_2 = \mu_2} \right] + O(y_{2t}^2) \right\}. \end{aligned} \quad (5.26)$$

Hence, for a system with an almost marginal scaling field the asymptotic critical exponent is only reached extremely close to the critical point (unless the amplitude of the transient vanishes). Outside that region the "exponent" appears to depend continuously on the scaling field  $\mu_2$ , and has to be interpreted as an effective exponent.

### C. Crossover phenomena in tricritical systems

Equations (3.3) with the exponents (3.4) are used to describe crossover phenomena in systems with a tricritical point, such as in He<sup>3</sup>-He<sup>4</sup> mixtures.<sup>17</sup> (Compare the discussion of approximations in Sec. III C.) In the present section we report the results of numerical calculations for the susceptibility  $\chi$ , the effective exponents  $\gamma_{\text{eff}}$  and  $\dot{\gamma}_{\text{eff}}$ , and the "flow diagram" in the scaling-field space. In these calculations we have approximated  $\bar{\chi}(\hat{\mu}_2)$  by a constant  $\bar{\chi} = 1$ , and chose  $h_2^* = 0.5$ . The departure of points  $(T, G)$  and  $(\mu_1, \mu_2)$ , respectively, from the critical line and the tricritical point is measured in terms of the quantities  $\mu_1$  and  $\rho(G)$  that were defined in Eqs. (3.20) and (3.22). We present only for the exponents (3.4) a complete set of figures.

First we consider the phase diagram in the  $(T, G)$  plane as shown in Fig. 2. We simulate an experiment by calculating for our model the susceptibility  $\chi$  of Eq. (4.8) and the effective exponent  $\gamma_{\text{eff}}(T, G)$  of Eq. (5.21) along paths of  $G = \text{const}$ , which approach the critical line at different distances  $\rho(G)$  from the tricritical point. Figure 3 shows a conventional double logarithmic plot of the susceptibility. The marked crossover region is the 3% crossover region defined by Eq. (5.16) with  $p = 0.03$ . The 25% crossover region is marked by two arrows. In general it is difficult to determine experimentally the true asymptotic critical exponents or even the existence of crossover phenomena by plotting data in this way. A scaling plot of the same data for  $\chi$  is shown in Fig. 4. This representation (in which  $\chi$  is divided by the leading singular behavior in one of the two asymptotic critical regions) allows a convenient experimental detection of crossover phenomena. (Compare also Fig. 6 of Ref. 15.) The best way to describe quantitatively crossover effects is by means of effective critical exponents. For  $\bar{\chi} = \text{const}$  Eq. (5.21) can be written as

$$\gamma_{\text{eff}} = \dot{\gamma}_{\text{eff}} \left[ 1 + \mu_1 \frac{d \mu_2}{d \mu_1} \frac{y_{1c} - y_{1t}}{y_{2t}} \left( \frac{\hat{\mu}_2}{\mu_2} - \frac{1 - \hat{\mu}_2}{1 - \mu_2} \right) \right] \quad (5.27)$$

by using Eq. (5.9). In Fig. 5 this effective exponent,  $\gamma_{\text{eff}}(T, G)$ , is plotted versus the logarithm of  $\mu_1(T, G) = 1 - T_c(G)/T$  for various values of  $\rho(G)$ . The effective exponent changes continuously from the asymptotic tricritical value  $\gamma_t = 1$  (far from the

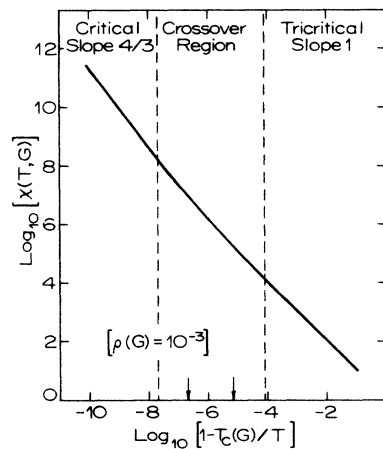


FIG. 3. Conventional double logarithmic plot of the susceptibility  $\chi$  taken along a path of constant  $\rho(G) = 10^{-3}$ . Outside the crossover region the slopes of the curve differ by less than 3% from their asymptotic values. The crossover region, allowing a 25% deviation from the asymptotic exponents, is marked by two arrows.

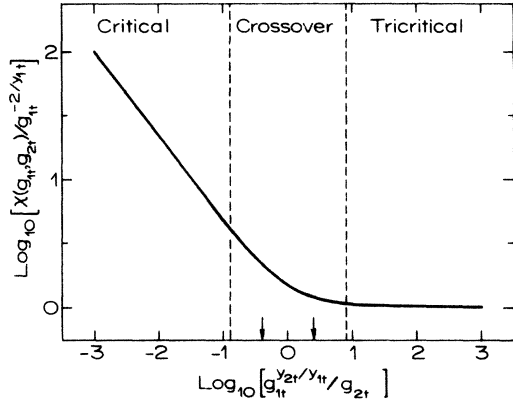


FIG. 4. Scaling representation of the susceptibility  $\chi$ . The tricritical scaling function  $v_t(c_t)$  defined in Eq. (4.9) is plotted versus the scaled temperature variable  $c_t = g_{1t}^{2t^1} g_{2t}^{-1} g_{2t}^{-1}$ . The crossover regions are defined as in Fig. 3. This representation of data allows a convenient detection of crossover phenomena.

critical line) to the asymptotic critical-line value  $\gamma_c = 1$  (close to the critical line). This crossover occurs the closer to the critical line the closer the path is to the tricritical path, i. e., the smaller  $\rho$ . The width of the 25% crossover region is about two decades in the relative temperature  $\mu_1$ , as expected from Eq. (5.17). [The bending of the effective exponents  $\gamma_{\text{eff}}(T, G)$  towards a common value as  $\mu_1 \rightarrow 1$  (i. e.,  $\beta \rightarrow 0$ ) is caused by the fact that in our model  $\mu_2 \rightarrow h_2^*$  becomes independent of  $G$  in that limit.] The results for  $\gamma_{\text{eff}}(T, G)$  allow us to divide the  $(T, G)$  plane in the neighborhood of the tricritical point into regions of different critical behavior, an asymptotic tricritical region and an asymptotic critical region, which are separated by a crossover region. This fact is important for the correct interpretation of laboratory experiments and computer experiments.

Next we discuss the effective exponent  $\dot{\gamma}_{\text{eff}}(\mu_1, \mu_2)$  of Eq. (5.12) and the flow diagram of the model in the  $(\mu_1, \mu_2)$  scaling-field space. The exponent  $\dot{\gamma}_{\text{eff}}$  describes the degree of singularity of  $\chi$  along paths of  $\mu_2 = \text{const}$ . The two important properties of this effective exponent are that it is constant along the trajectories  $\hat{\mu}_2(\mu_1, \mu_2) = \text{const}$  and that it “scales,” i. e., that  $\dot{\gamma}_{\text{eff}} = \dot{\gamma}_{\text{eff}}(C)$ , according to Eq. (5.3). The  $\hat{\mu}_2$  trajectories are determined by Eqs. (4.5) and (4.10) and are plotted in Fig. 6. The trajectories  $\hat{\mu}_{2,t} = 0.25$  and  $\hat{\mu}_{2,c} = 0.75$  bound the 25% crossover region. The asymptotic tricritical region is defined to be the area of the scaling-field space with  $\hat{\mu}_2 < \hat{\mu}_{2,t}$ , and the asymptotic critical region the area  $\hat{\mu}_2 > \hat{\mu}_{2,c}$ . The trajectory  $\hat{\mu}_2 = 0$  leaves the tricritical fixed point  $(0, 0)$  along the  $\mu_1$  axis, and the trajectory  $\hat{\mu}_2 = 1$  leaves the critical

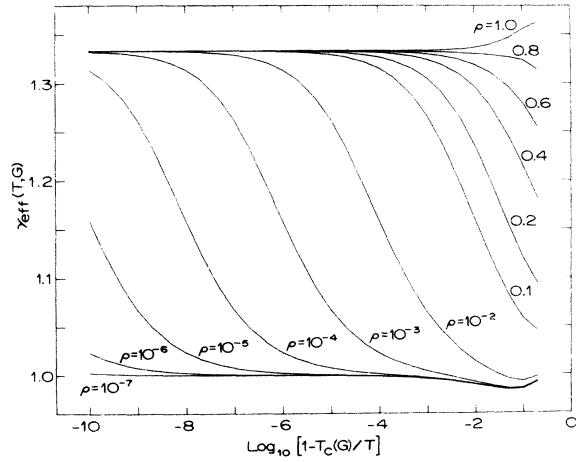


FIG. 5. Effective exponents  $\gamma_{\text{eff}}(T, G)$  for a tricritical system with the asymptotic exponents  $\gamma_{1c} = 1.5$ ,  $\gamma_{1t} = 2$ ,  $\gamma_{2t} = 1$ . The parameter  $\rho$  specifies the path of approach to criticality as defined in Figs. 1 and 2. The width of the 25% crossover region is about two decades in the relative temperature.

fixed point  $(0, 1)$  parallel to the  $\mu_1$  axis. In Fig. 6 we also present lines of  $\hat{l}(\mu_1, \mu_2) = \text{const}$ , which can be obtained from Eqs. (3.8a) and (3.14) or (4.1)–(4.5). It is instructive to represent the experimental paths  $G = \text{const}$  in the flow diagram of Fig. 6 and to study the crossover phenomena along these paths by observing which  $\hat{\mu}_2$  trajectories they cross. [Figure 1 includes several paths  $\rho(G) = \text{const}$ .] The effective exponent  $\dot{\gamma}_{\text{eff}}(\mu_1, \mu_2)$  scales and is only a

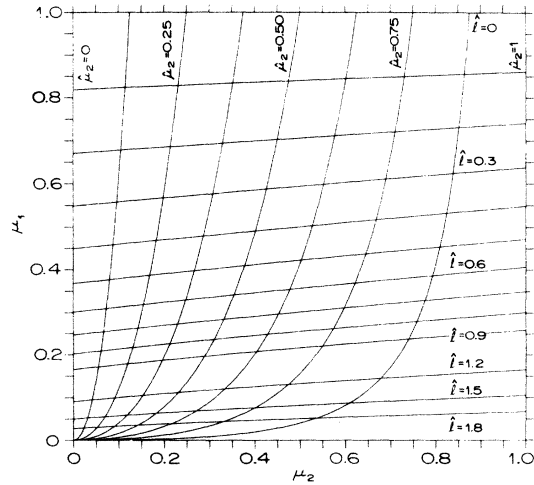


FIG. 6. Flow diagram in the scaling-field space for the tricritical system. The diagram is discussed in Secs. V C and IV B of the text.

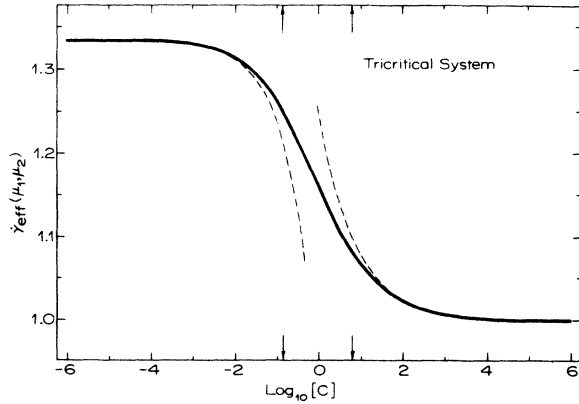


FIG. 7. Scaling representation of the effective exponent  $\dot{\gamma}_{\text{eff}}(\mu_1, \mu_2)$  for the tricritical system. The exponent is plotted versus the logarithm of the scaling variable  $C$  defined in Eq. (4.5). The 25% crossover region is marked by two arrows. The dashed curves are the results for the approximate effective exponents of Eqs. (5.13). The approximations give a good estimate outside the crossover region.

function of the scaled relative temperature  $C$  of Eq. (4.5). A scaling plot for  $\dot{\gamma}_{\text{eff}}$  is shown in Fig. 7, together with the approximate effective exponents  $\dot{\gamma}_{\text{eff}}$  in the asymptotic tricritical and critical regions (dashed curves) obtained from Eqs. (5.13). The approximate formulas yield good estimates for  $\dot{\gamma}_{\text{eff}}$  outside the crossover region. Figure 5 shows that the effective exponents  $\gamma_{\text{eff}}(T, G)$  do not scale exactly. This is a consequence of the  $(d\mu_2/d\mu_1)$  term in Eq. (5.21), which is present if one studies crossover phenomena along the experimental paths  $G = \text{const}$ .

#### D. Ashkin-Teller model

The Ashkin-Teller model in  $d = 3$  dimensions is characterized by the asymptotic indices (3.6). (Compare also Appendix A.) Therefore, the crossover phenomena in an Ashkin-Teller system are qualitatively the same as in the tricritical system studied in the last paragraph. The difference is that they occur on a completely different scale. With the exponents (3.6) we find for the width of the 25% crossover region  $W_{\text{CR}}(0.25) \approx 10^9$ , i. e., a width that is a factor  $10^7$  larger than the crossover width for the tricritical system (3.4).<sup>28</sup> This demonstrates the dependence of crossover effects on the value of the crossover exponent.

Based on series-expansion studies it has been recently suggested<sup>18</sup> that the Ashkin-Teller model in  $d = 3$  dimensions might violate the universality principle (such as the two-dimensional Ashkin-Teller model, which resembles the Baxter mod-

el<sup>27</sup>). Our result for the width of the crossover region implies that it is practically impossible to obtain the asymptotic critical exponents by series-expansion techniques, and thus to make statements on the universality hypothesis. We will return to this question in Sec. VII.

Results for the effective exponent  $\gamma_{\text{eff}}(T, G)$  defined by Eq. (5.21) are shown in Fig. 8. The changeover from the tricritical behavior to the critical-line behavior occurs very gradually over about nine decades in the relative temperature. (Note that in this figure the scale of the abscissa has been reduced by a factor  $\frac{1}{4}$  compared to Fig. 5.) Since the crossover exponent is small the approximate formula (5.26) for  $\dot{\gamma}_{\text{eff}}(\mu_1, \mu_2)$  can be used to estimate the effective exponent. Therefore, for not too small  $\mu_1$ , a leading term  $\gamma(\mu_2) = 2/y_{1,\text{eff}}(\mu_2)$  exists, which varies continuously with the irrelevant scaling field  $\mu_2$ . The slope of this exponent is

$$\begin{aligned} \frac{\partial \gamma(\mu_2)}{\partial \mu_2} &= -\frac{1}{2}(y_{1c} - y_{1t})\gamma^2(\mu_2) \\ &\approx -0.3\gamma^2(\mu_2), \end{aligned} \quad (5.28)$$

with  $\gamma(\mu_2)$  varying between 0.91 and 1.25, which describes qualitatively Ditzian's conclusions.<sup>18</sup>

It is instructive to compare the flow diagrams in Figs. 9 and 6. For the Ashkin-Teller model the trajectories  $\hat{\mu}_2$  have a very large slope for not too small  $\mu_1$  and bend towards the tricritical fixed point only very close to the "critical line," which connects the tricritical fixed point (0, 0) and the critical fixed point (0, 1). This behavior is char-

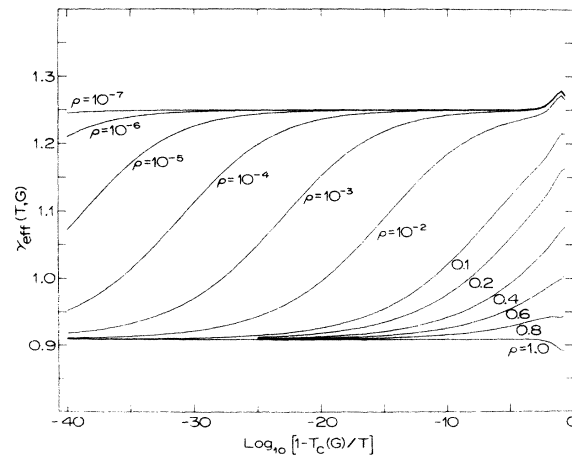


FIG. 8. Effective exponent  $\gamma_{\text{eff}}(T, G)$  for the Ashkin-Teller model in three dimensions with the asymptotic exponents  $y_{1c} = 2.2$ ,  $y_{1t} = 1.6$ ,  $y_{2t} = 0.2$ . The parameter  $\rho$  defines the path of approach to criticality.

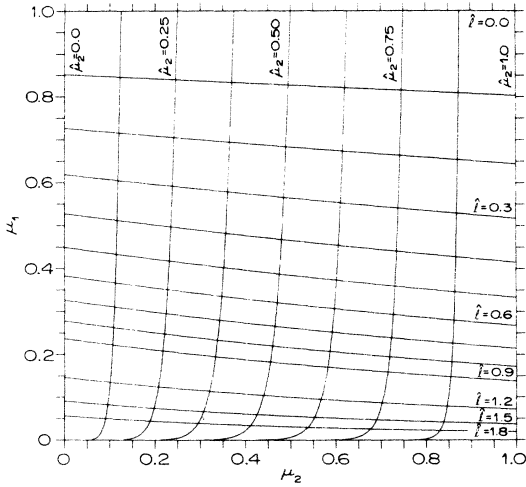


FIG. 9. Flow diagram in the scaling-field space for the tricritical and critical phase transitions of the Ashkin-Teller model in three dimensions.

acteristic for crossover phenomena with very small crossover exponents or slow transients. It shows that the critical region is very narrow and that the asymptotic critical behavior is approached extremely slowly.

## VI. FISHER EXPONENT RENORMALIZATION

In this section we show that the Fisher exponent renormalization<sup>13</sup> is a crossover phenomenon that is described by the model equations (3.3) with the exponents (3.7). Therefore, all results of Secs. IV and V, subject only to a redefinition of the scaling fields and indices, apply to this case.

We consider a system with the thermodynamic potential  $F$  which depends on three experimental fields: the temperature  $T$ , an irrelevant field  $G$ , and the field  $H$  that couples to the "order parameter." Near criticality the potential  $F$  can be written in a scaled form,

$$F = F(g_0, g_1, g_h) = g_0 + g_1^{d/y_1} f(g_h/g_1^{y_h/y_1}), \quad (6.1)$$

where the  $g$ 's are scaling fields. The field  $g_0$  represents the analytic contribution to  $F$ , the field  $g_1$  measures the departure of the system from the critical line  $T_c(G)$  in the  $(T, G)$  plane, and  $g_h$  is the symmetry-breaking scaling field. (It is assumed that the transition occurs at  $H=0$ .) We assume that both  $g_0$  and  $g_1$  are smooth functions of  $T$  and  $G$ ,

$$g_0 = g_0(T, G), \quad g_1 = g_1(T, G). \quad (6.2)$$

The phase transition observed at constant field  $G$  is assumed to be governed by the ordinary, asymptotic scaling indices

$$y_1 = d/(2-\alpha), \quad y_h = \frac{1}{2}(d+2-\eta). \quad (6.3)$$

The ratio  $y_h/y_1 = \Delta$  is the "gap exponent." Equation (6.1) with  $\eta=0$  yields  $\chi = g_1^{-2/y_1} f''(0)$  for the susceptibility in zero field  $H$ . This result can be written in a form similar to Eq. (3.30),

$$\chi(g_1, 0) = e^{2\hat{t}} f''(0) \quad \text{with} \quad g_1 = e^{-y_1 \hat{t}}. \quad (6.4)$$

Fisher-renormalized critical exponents characterize the transition in a region close to the critical temperature if the transition is observed at constant density  $X = -\partial F/\partial G$  instead of at constant field  $G$ . We write the constraint in the form<sup>36</sup>

$$X = X(T, G) = -\frac{\partial F}{\partial G} = -\frac{\partial g_0}{\partial G} - (\text{const}) (2-\alpha) \frac{\partial g_1}{\partial G} g_1^{1-\alpha}. \quad (6.5)$$

Now we solve  $g_1 = g_1(T, G)$  in Eq. (6.2) for  $G = G(g_1, T)$ , and expand  $\partial g_1/\partial G$  into powers of  $g_1$ :

$$-\frac{\partial g_0}{\partial G} = P_0(T) + g_1 P_1(T) + O(g_1^2), \quad (6.6)$$

$$-(\text{const}) (2-\alpha) \frac{\partial g_1}{\partial G} = P_2(T) + O(g_1). \quad (6.7)$$

Then Eq. (6.5) for the constraint becomes

$$X - P_0(T) = g_1 P_1(T) + g_1^{1-\alpha} P_2(T), \quad (6.8)$$

which can be written in the form

$$\tau = g_1(1-\nu) + g_1^{1-\alpha} \nu \quad (6.9)$$

by introducing the reduced variables

$$\tau = \frac{X - P_0(T)}{P_1(T) + P_2(T)}, \quad \nu = \frac{P_2(T)}{P_1(T) + P_2(T)}. \quad (6.10)$$

These results can be interpreted in terms of the scaling-field approach to crossover phenomena. The critical temperature is defined by  $g_1(T, G) = 0$ ; hence

$$P_0(T_c(X)) = X. \quad (6.11)$$

Therefore, the field  $\tau$  in Eq. (6.10) is proportional to the relative temperature  $T - T_c(X)$ , and characterizes the departure of the constrained system from criticality. We note that the metric (scale of  $\tau$ , etc.) is determined by the details of the functions  $P(T)$ . From Eq. (6.9) we find that  $g_1 = \tau$  for  $\nu=0$  and  $g_1 = \tau^{1/(1-\alpha)}$  for  $\nu=1$ . Hence  $\nu$  plays the role of an irrelevant field and determines the crossover from the unrenormalized exponent  $\gamma = 2/y_1$ , when  $\nu \ll 1$ , to the Fisher renormalized exponent  $\gamma^{(X)} = 2/y_{1X} = \gamma/(1-\alpha)$ , when  $\nu \approx 1$ . Thus, in addition to the indices (6.3) we can introduce two other asymptotic indices, the Fisher-renormalized index  $y_{1X}$  and the crossover index  $y_\phi$ , which are given by

$$y_{1X} = \frac{d(1-\alpha)}{2-\alpha}, \quad y_\phi = \frac{d\alpha}{2-\alpha}. \quad (6.12)$$

We expect that the indices  $y_{1x}$ ,  $y_1$ , and  $y_\phi$  play for the Fisher renormalization the same role as the indices  $y_{1c}$ ,  $y_{1t}$ , and  $y_{2t}$  for the tricritical crossover phenomena. By making the substitutions

$$\tau \rightarrow \mu_1, \quad \nu \rightarrow \mu_2, \quad (6.13a)$$

$$y_{1x} \rightarrow y_{1c}, \quad y_1 \rightarrow y_{1t}, \quad y_\phi \rightarrow y_{2t} \quad (6.13b)$$

in the boundary condition (3.28), or equivalently in Eqs. (4.1)–(4.5), and by observing that now  $e^{-y_1} = g_1$ , we obtain exactly the constraint equation (6.9). Therefore, the Fisher exponent renormalization (in this approximation) is precisely described by our crossover scaling-field equations (3.3).

Hence the results for the susceptibility  $\chi$  and the effective exponents  $\gamma_{\text{eff}}$  that were derived in Secs. IV and V for tricritical systems apply also to systems with Fisher renormalization due to a constraint [with the identifications (6.13)]. Of particular interest are the scaling function for the susceptibility  $\chi(\tau, \nu)$ , given by Eq. (4.8) or (4.9), and the effective exponent  $\gamma_{\text{eff}}^{(X)}(\tau, \nu)$  given by Eq. (5.21). Numerical results for  $\gamma_{\text{eff}}^{(X)}$  with the asymptotic exponents (3.7) are shown in Fig. 10. By applying the definition (5.16) for the width of crossover regions to the crossover region  $\gamma$  to  $\gamma^{(X)}$ , we find for the corresponding 25% crossover region

$$W_{\text{CR}}(0.25) = 3^{(2-\alpha)/\alpha}. \quad (6.14)$$

For decorated Ising models with  $\alpha = \frac{1}{8}$  this width is approximately  $W_{\text{CR}} \approx 3 \times 10^6$ , in agreement with the result in Fig. 10. The size of the inner, i. e.,

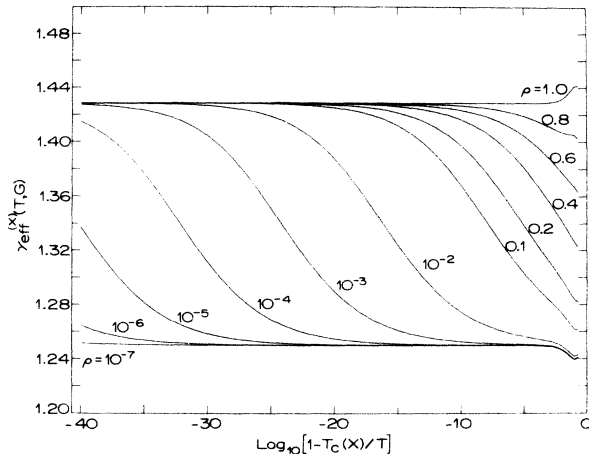


FIG. 10. Effective exponents  $\gamma_{\text{eff}}^{(X)}(T, G)$  for a system exhibiting Fisher exponent renormalization due to a constraint. The asymptotic exponents  $y_x = 1.4$ ,  $y_1 = 1.6$ , and  $y_\phi = 0.2$  are those of the decorated Ising model. The crossover occurs from the Ising exponent  $\gamma = 2/y_1$  to the Fisher-renormalized exponent  $\gamma^{(X)} = 2/y_{1x}$ . The crossover exponent  $y_\phi$  determines the width of the 25% crossover region  $W_{\text{CR}}(0.25) \approx 3 \times 10^6$ .

Fisher-renormalized region can be estimated from Eq. (5.15). The large width of the crossover region makes it probably impossible to observe experimentally the complete crossover between the asymptotic critical exponents  $\gamma$  and  $\gamma^{(X)}$ .<sup>13,19</sup> It is more sensible to determine also experimentally effective exponents and to try to detect the onset of the crossover. Since the crossover exponent  $y_\phi \approx 0.2$  is small the effective exponent  $\gamma_{\text{eff}}^{(X)}(\tau, \nu)$  can be approximated by Eq. (5.26), i. e.,

$$\gamma_{\text{eff}}^{(X)}(\tau, \nu) = \frac{2}{y_{1,\text{eff}}(\nu)} \left[ 1 + \left( \frac{y_\phi}{y_{1,\text{eff}}(\nu)} \right)^2 \times \nu(1-\nu) \ln(1/\tau) + \dots \right], \quad (6.15)$$

with  $y_{1,\text{eff}}(\nu) = y_1 + \nu(y_{1x} - y_1)$  in the region  $\tau \gg \exp[-y_{1,\text{eff}}(\nu)/(1-\nu)y_\phi]$ . Hence it deviates only for small  $\tau$  from an effective exponent  $\gamma^{(X)}(\nu) = 2/y_{1,\text{eff}}(\nu)$ . The "flow diagram" (lines of constant  $\mu_2$  and  $\hat{l}$ ) in the  $(\tau, \nu)$  plane for the constrained system is very similar to Fig. 9 for the Ashkin-Teller model. The only difference is that the lines of  $\hat{l} = \text{const}$  have a small positive slope here because  $y_{1x} < y_1$ .

## VII. EFFECTIVE EXPONENTS AND SERIES EXPANSIONS

Series-expansion techniques have been widely used to estimate the asymptotic values of critical exponents from the first  $n$  terms of power-series expansions for thermodynamic and correlation functions.<sup>1</sup> In this section we show that the method can easily lead to wrong conclusions for systems with crossover effects due to competing critical instabilities. We define effective critical exponents as functions of the number of terms of series expansions, and study the kind of information that can be obtained from  $n$  terms of such series.

### A. Effective exponents from series expansions

First we describe the results of numerical calculations. We start from the explicit expressions (4.8) and (4.9) for the susceptibility  $\chi$  and expand around  $\mu_1 = 1$ ,

$$\chi = \sum_{n=0}^{\infty} a_n x^n \quad \text{with } x = 1 - \mu_1. \quad (7.1)$$

An effective exponent  $\gamma_{\text{eff}}(n)$  depending on the number of terms included in the expansion (7.1) is then defined by the ratio method,<sup>1</sup>

$$\gamma_{\text{eff}}(n) = 1 + n \left( \frac{a_n}{a_{n-1}} - 1 \right). \quad (7.2)$$

In general, the effective exponent  $\gamma_{\text{eff}}(n)$  is also a function of the nonordering field  $G$ , or, in our convention, of  $\rho(G)$ , i. e.,  $\gamma_{\text{eff}}(n) = \gamma_{\text{eff}}(n, \rho)$ . This result is not in contradiction to the universality hypothesis, which states that the asymptotic critical exponents are independent of irrelevant variables.<sup>37</sup>

Exact coefficients  $a_n$  in the expansion (7.1) were obtained numerically by solving Eqs. (4.1)–(4.4) to order  $n$  in  $x = 1 - \mu_1$  and substituting the results into Eq. (3.30). Figures 11–13 show the effective exponents  $\gamma_{\text{eff}}(n, \rho)$ , for various values of  $\rho$ , as functions of  $1/n$  (in the interval  $n = 3, \dots, 20$ ) for the tricritical system with the asymptotic indices (3.4), the Ashkin–Teller system with the indices (3.6), and the Fisher constrained system with the indices (3.7). (As in Sec. V we choose  $\bar{\chi} = 1$  and  $h_2^* = 0.5$ .)

The most striking result is that the effective exponents  $\gamma_{\text{eff}}(n, \rho)$  appear to depend strongly on the irrelevant field  $\rho$  and only *weakly* on the parameter  $n$ . From Fig. 11 we conclude that we can probe with  $n = 20$  terms the asymptotic critical region only when  $\rho \geq 0.5$ . The universality principle (which is built into our model) requires that  $\gamma_{\text{eff}}(n, \rho)$  approaches, in the limit  $n \rightarrow \infty$ , the asymptotic value  $\gamma_c = \frac{4}{3}$  for all  $\rho > 0$ . Figure 11 shows that it becomes increasingly difficult to draw that conclusion from calculations of  $\gamma_{\text{eff}}(n, \rho)$  based on only 20 terms, if the critical line is approached along paths with  $\rho < 0.5$ . This result is obvious from the location of the crossover area shown in Figs. 1 and 6. To get a rough idea of the temperature region that is probed by  $n = 20$  terms of the expansion one may compare the values of the effective exponents in Figs. 5 and 11.<sup>38</sup> [For

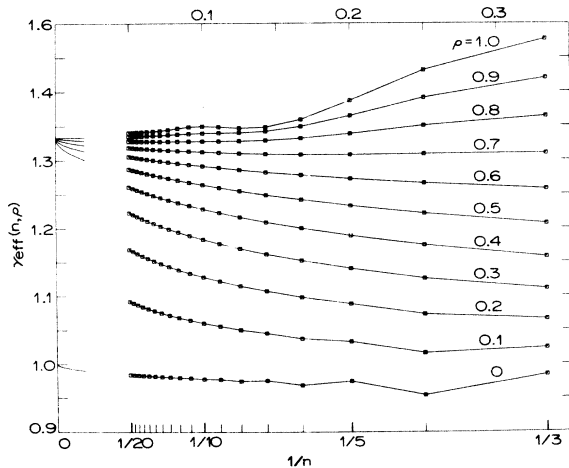


FIG. 11. Series-expansion data for the effective exponent  $\gamma_{\text{eff}}(n, \rho)$  of the tricritical system as a function of the inverse of the number of terms  $n$  included in the series. The parameter  $\rho$ , which defines the path of approach to criticality, is defined in Figs. 1 and 2. For all  $\rho > 0$  the asymptotic value of the exponent in the limit  $1/n \rightarrow 0$  is  $\gamma_c = \frac{4}{3}$ . The figure demonstrates that this fact is difficult to confirm by a series of only 20 terms. The results for  $\gamma_{\text{eff}}$  for small  $1/n$  and  $\rho = 1, 0.9, 0.8, 0.7, 0.6$ , and  $0.0$  are obtained from Eqs. (7.7) and (7.12).

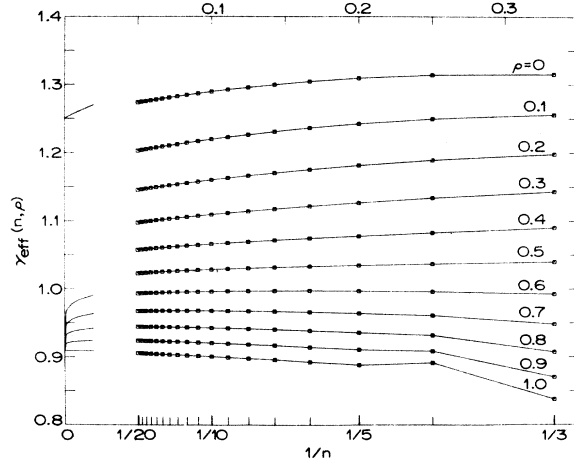


FIG. 12. Effective exponent  $\gamma_{\text{eff}}(n, \rho)$  versus  $1/n$  for the Ashkin–Teller model in three dimensions. The parameter  $\rho$  is defined in Fig. 2. Based on a series of 20 terms it is impossible to draw conclusions on the validity of the universality principle for this model. The exponents in the limit  $1/n \rightarrow 0$  are obtained from Eqs. (7.7) and (7.12).

example, along the path  $\rho = 0.1$  the temperature-dependent effective exponent  $\gamma_{\text{eff}}$  at about  $\mu_1 = 4 \times 10^{-2}$ . However, the 10% crossover to the asymptotic critical behavior ( $\gamma_{\text{eff}} \approx 1.30$ ) is only completed two decades closer to criticality at  $\mu_1 = 3 \times 10^{-4}$ .) The effective exponents  $\gamma_{\text{eff}}(n, \rho)$  in Figs. 12 and 13 for the Ashkin–Teller model and the Fisher constrained system show qualitatively the same

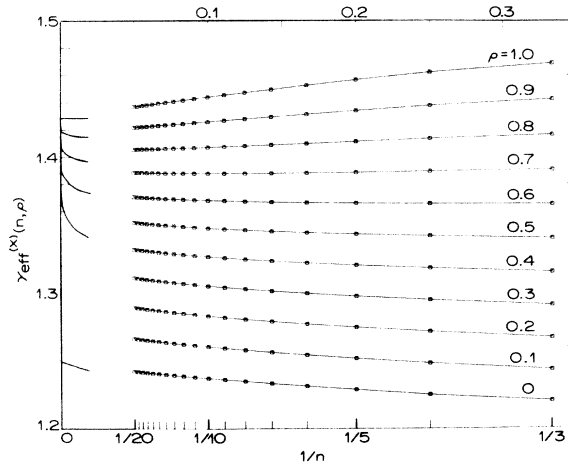


FIG. 13. Effective exponent  $\gamma_{\text{eff}}^{(x)}(n, \rho)$  versus  $1/n$  for a decorated Ising system exhibiting Fisher exponent renormalization. The parameter  $\rho$  is defined in Fig. 2. The series of 20 terms does not show the convergence of the effective exponents (for  $\rho > 0$ ) towards their asymptotic value  $\gamma^{(x)} = 1.43$  at  $1/n = 0$ . The effective exponents in the asymptotic  $1/n$  region are calculated from Eqs. (7.7) and (7.12).

behavior as Fig. 11. Quantitatively the effective exponents exhibit an even weaker dependence on the parameter  $n$ . The result in Fig. 12 makes it understandable that the validity of the universality principle for the Ashkin-Teller model could not be deduced from relatively short series for the exponent  $\gamma$ .<sup>18</sup>

### B. Asymptotic formulas for effective exponents

The effective exponent  $\gamma_{\text{eff}}(n, \rho)$  can be discussed in analogy to the approach to  $\gamma_{\text{eff}}(T, G)$  in Sec. V. Given a path of  $G = \text{const}$ , there are two questions of interest. What is the size of the crossover region as a function of  $1/n$ ? How many terms of a series expansion are necessary to determine the true asymptotic critical exponent? Here we will only discuss a third question: the convergence of the effective exponent  $\gamma_{\text{eff}}(n, \rho)$  for large  $n$  towards  $\gamma_c$  or  $\gamma_t$  as a function of the crossover exponent that governs the competition between the two fixed points. In this paragraph we consider the case  $\phi_t < 1$ , i. e.,  $y_{2t} < y_{1t}$ . The examples discussed in the preceding sections fall into that category. In Sec. VIIC we comment on the case  $\phi_t > 1$ , which is relevant for the crossover in anisotropic classical spin systems.

Asymptotic formulas for the effective exponent  $\gamma_{\text{eff}}(n, \rho)$  can be derived by starting from the expansions (4.15) and (4.17) for  $\chi$ . We evaluate these exponents along paths  $\rho(G) = \text{const}$ , i. e.,  $\mu_2 = \rho + r\mu_1$  in the scaling-field space as shown in Fig. 1. In the critical region  $c_c \ll 1$  along  $\mu_2 = \rho + r\mu_1$  we obtain from Eq. (4.17) the leading terms

$$\chi \propto \mu_1^{-\gamma_c} [1 - A_c(\rho) \mu_1^{|\phi_c|} + O(\mu_1, \mu_1^{2|\phi_c|})], \quad (7.3)$$

with the exponents  $\gamma_c$  and  $\phi_c$  defined in Eq. (4.12b) and the amplitude

$$A_c(\rho) = \left( \frac{2\sigma_c}{y_{2t}} + \frac{\partial \ln \bar{\chi}}{\partial \hat{\mu}_2} \Big|_{\hat{\mu}_2=1} \right) (1 - \rho) \rho^{-y_{1t}/y_{1c}}. \quad (7.4)$$

The  $n$ th binomial coefficient of the expansion of  $(1-x)^{-\gamma}$  is

$$(-1)^n \binom{-\gamma}{n} \simeq \frac{n^{\gamma-1}}{\Gamma(\gamma)} \quad \text{when } n \rightarrow \infty. \quad (7.5)$$

In this approximation we obtain

$$a_n \propto \frac{n^{\gamma_c-1}}{\Gamma(\gamma_c)} \left[ 1 - A_c(\rho) \frac{\Gamma(\gamma_c)}{\Gamma(\gamma_c + \phi_c)} n^{-|\phi_c|} + O(n^{-1}, n^{-2|\phi_c|}) \right], \quad (7.6)$$

or, by using Eq. (7.2),

$$\gamma_{\text{eff}}(n, \rho) = \gamma_c + A_c(\rho) \frac{|\phi_c| \Gamma(\gamma_c)}{\Gamma(\gamma_c + \phi_c)} n^{-|\phi_c|} + O(n^{-1}, n^{-2|\phi_c|}) \quad (7.7)$$

for all  $n$  satisfying

$$n^{|\phi_c|} \gg (1 - \rho) \rho^{-\gamma_c/\gamma_t}. \quad (7.8)$$

Therefore, if the confluent singularities in  $\chi$  differ by a small crossover exponent,  $|\phi_c| \ll 1$ , then the effective exponent  $\gamma_{\text{eff}}(n, \rho)$  approaches the asymptotic value  $\gamma_c$  very slowly. That is, for example, the case in the Ashkin-Teller model in three dimensions. With the set of exponents (3.6) we obtain the equation

$$\gamma_{\text{eff}}(n, \rho) = 0.91 + 0.23(1 - \rho) \rho^{-0.727} n^{-0.091} + O(n^{-0.182}), \quad (7.9)$$

which describes well the  $\rho$  dependence of the effective exponent in Fig. 12. In Figs. 11 and 13, improved matching between the asymptotic and exact series expansion results can be achieved by including the next correction term to Eq. (7.7) which is of the order  $n^{-1}$ .

An asymptotic formula for the effective exponent  $\gamma_{\text{eff}}(n, \rho)$  in the tricritical region  $c_t \ll 1$  can be similarly derived by starting from Eq. (4.15). For small nonzero  $\rho$  one obtains

$$\gamma_{\text{eff}}(n, \rho) = \gamma_t + A_{1t}(\rho) \frac{\phi_t \Gamma(\gamma_t)}{\Gamma(\gamma_t + \phi_t)} n^{\phi_t} + \dots, \quad (7.10a)$$

with the amplitude

$$A_{1t}(\rho) = \left( \frac{2\sigma_t}{y_{2t}} + \frac{\partial \ln \bar{\chi}}{\partial \hat{\mu}_2} \Big|_{\hat{\mu}_2=0} \right) (1 - \rho)^{-y_{1c}/y_{1t}} \rho, \quad (7.10b)$$

in the region

$$n \gg 1 \quad \text{and} \quad n^{\phi_t} \ll (1 - \rho)^{\gamma_t/\gamma_c} \rho^{-1}. \quad (7.11)$$

For the tricritical path  $\mu_2 = r\mu_1$  [with  $r = h_2^*$ , compare Eq. (3.22)] the amplitude  $A_{1t}$  vanishes and the first correction to  $\gamma_t$  becomes of the order  $n^{\phi_t-1}$ ,

$$\gamma_{\text{eff}}(n, 0) = \gamma_t + A_{2t}(0) \frac{(\phi_t - 1) \Gamma(\gamma_t)}{\Gamma(\gamma_t + \phi_t - 1)} n^{\phi_t-1} + O(n^{-1}, n^{2(\phi_t-1)}), \quad (7.12a)$$

with

$$A_{2t}(0) = \left( \frac{2\sigma_t}{y_{2t}} + \frac{\partial \ln \bar{\chi}}{\partial \hat{\mu}_2} \Big|_{\hat{\mu}_2=0} \right) r. \quad (7.12b)$$

For the tricritical system with the indices (3.4) and  $r = 0.5$ , for example, Eqs. (7.12) lead to

$$\gamma_{\text{eff}}(n, 0) = 1 - 0.0705 n^{-0.5} + O(n^{-1}), \quad (7.13)$$

which yields  $\gamma_{\text{eff}}(20, 0) \approx 0.984$ , in good agreement with the result of exact series expansion in Fig. 11.

Effective exponents  $\dot{\gamma}_{\text{eff}}(n, \mu_2)$  along paths  $\mu_2 = \text{const}$  can be similarly defined. Up to corrections of order  $1/n$  these exponents scale

$$\dot{\gamma}_{\text{eff}}(n, \mu_2) = \dot{\gamma}_{\text{eff}}[n^{-|\phi_c|} (1 - \mu_2) \mu_2^{-\gamma_c/\gamma_t}] \times [1 + O(n^{-1})], \quad (7.14)$$

which is analogous to the result in Eq. (5.3). Moreover, if the scaling field  $\mu_2$  is almost marginal, that is if  $y_{2t} \ll 1$ , then we find in analogy to Eq. (5.26) that

$$\dot{\gamma}_{\text{eff}}(n, \mu_2) = \gamma_{\text{eff}}(\mu_2) + \dot{A}(\mu_2)(\ln n) + O(y_{2t}^2), \quad (7.15a)$$

where  $\gamma_{\text{eff}}(\mu_2)$  is given by Eq. (5.23) and  $\dot{A}(\mu_2)$  is the amplitude,

$$\dot{A}(\mu_2) = \frac{1}{4} y_{2t} (y_{1t} - y_{1c}) \mu_2 (1 - \mu_2) \gamma_{\text{eff}}^3(\mu_2). \quad (7.15b)$$

This result demonstrates again the very weak dependence of effective exponents on the number of terms  $n$  of series expansions if the crossover exponent is small. Equation (7.15) can be used to estimate  $\gamma_{\text{eff}}(n, \rho)$ , as described in Sec. VD.<sup>39</sup>

The results in this section show that the size of the crossover exponent determines the degree of convergence of the effective exponents  $\gamma_{\text{eff}}(n)$  towards their asymptotic values. This fact indicates the limitations of the series-expansion method for systems with crossover phenomena.

### C. Crossover phenomena with $\phi_t > 1$

Classical anisotropic spin systems are characterized by crossover exponents larger than 1.<sup>14</sup> The set of critical indices describing competing fixed points of the Heisenberg-type and the Ising-type is

$$y_{1c} = 1.60, \quad y_{1t} = 1.45, \quad y_{2t} = 1.81, \quad (7.16)$$

which yields  $\phi_t = y_{2t}/y_{1t} = 1.25$ .<sup>40</sup> Although our model equations do not adequately describe anisotropic spin systems we will use the equations here to discuss some features of crossover phenomena with  $\phi_t > 1$ . We continue to refer to the two competing fixed points as the tricritical fixed point and the critical fixed point (instead of naming them isotropic and anisotropic).

Figure 14 shows, for a system with the indices (7.16), the effective exponent  $\gamma_{\text{eff}}(n, \rho)$  as a function of  $1/n$  for several values of  $\rho$ . All paths with  $\rho > 0$  approach the critical line, which exhibits Ising-like critical behavior. The curves for  $\gamma_{\text{eff}}(n, \rho)$  show a *pronounced* bending towards the asymptotic Ising value  $\gamma_c = 1.25$ . This good convergence of the effective exponent towards its asymptotic value contrasts with the *weak*  $n$  dependence of the exponents in Figs. 11–13. It is a consequence of the large value of the crossover exponent, which here leads to a 25% crossover region with a width of about one decade in the reduced temperature. (Hence, series expansion techniques can be very useful for the study of crossover phenomena in the anisotropic Heisenberg model as was shown by Jasnow and Wortis.<sup>41</sup>) The path  $\rho = 0$ , i. e.,  $\mu_2 = r\mu_1$  with  $r = \bar{n}_2^*$ , approaches the tricritical fixed

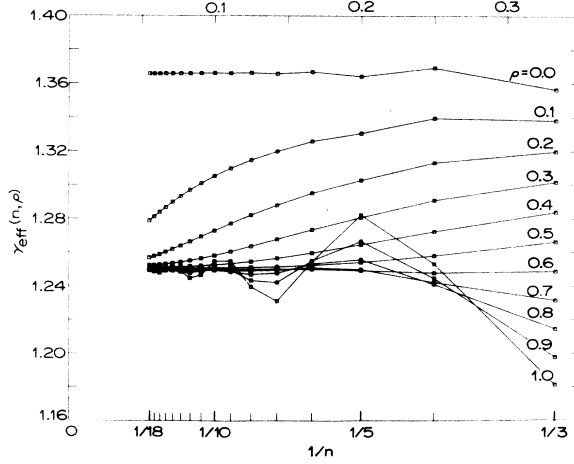


FIG. 14. Effective exponents  $\gamma_{\text{eff}}(n, \rho)$  versus  $1/n$  for a system with the asymptotic scaling indices (7.16). The curves for the effective exponents along all paths approaching the critical line bend towards the asymptotic value  $\gamma_c = 1.25$ .

point. We notice from Fig. 14 that the curve for  $\gamma_{\text{eff}}(n, 0)$  does not extrapolate to the Heisenberg exponent  $\gamma_t = 1.38$ . How can the deviation be explained? From Eq. (4.17) we find for  $\mu_2 = r\mu_1 \ll 1$  the expansion

$$\chi \propto \mu_1^{-\tilde{\gamma}} [1 - \bar{A} \mu_1^{\tilde{\phi}} + O(\mu_1^{2\tilde{\phi}})], \quad (7.17)$$

with the exponents

$$\tilde{\gamma} = \frac{2}{y_{1c}} + \frac{2\sigma_c}{y_{2t}}, \quad \tilde{\phi} = \frac{y_{2t} - y_{1t}}{y_{1c}} \quad (7.18a)$$

and the amplitude

$$\bar{A} = \left( \frac{2\sigma_c}{y_{2t}} + \frac{\partial \ln \bar{\chi}}{\partial \mu_2} \Big|_{\mu_2=1} \right) r^{-y_{1t}/y_{1c}}. \quad (7.18b)$$

As in Eqs. (7.5)–(7.7) we find the effective exponent

$$\gamma_{\text{eff}}(n, 0) = \tilde{\gamma} + \bar{A} \frac{\tilde{\phi} \Gamma(\tilde{\gamma})}{\Gamma(\tilde{\gamma} - \tilde{\phi})} n^{-\tilde{\phi}} + O(n^{-2\tilde{\phi}}). \quad (7.19)$$

With the set of exponents (7.16) and  $r = 0.5$ , this leads to

$$\gamma_{\text{eff}}(n, 0) = 1.354 + 0.041 n^{-0.225} + O(n^{-0.45}), \quad (7.20)$$

which for  $n = 18$  yields  $\gamma_{\text{eff}}(18, 0) \approx 1.375$ , in agreement with the result in Fig. 14. In the limit  $n \rightarrow \infty$  neither the tricritical exponent  $\gamma_t$  nor the critical exponent  $\gamma_c$  is approached but  $\tilde{\gamma} = 1.354$ . Figure 15 gives the clue to this behavior. Because of  $\phi_t > 1$  the shape of the crossover region differs from the one in Fig. 1. [The latter figure is drawn for a system with the exponents (3.4).] The tricritical path, although confined to the crossover region for all practical purposes, approaches the tricritical

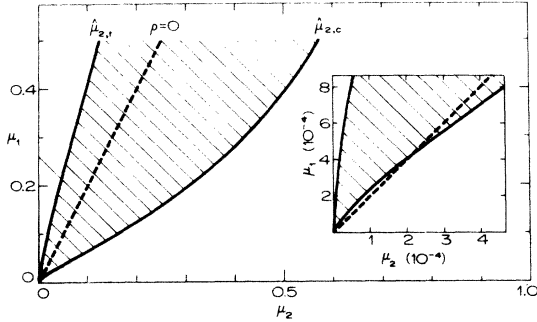


FIG. 15. Phase diagram in the  $(\mu_1, \mu_2)$  scaling-field plane for a system with a crossover exponent  $\phi_t > 1$ . The competing fixed points are located at  $(0, 0)$  and  $(0, 1)$ . The shaded area denotes the crossover region; its shape differs from the shape of the crossover region in Fig. 1. The effective exponent  $\gamma_{\text{eff}}(\mu)$  along the "tricritical" path  $\rho = 0$  is discussed in the text.

fixed point finally through the critical region as the insert in the figure shows. In other words, for this path the amplitude exponent  $-2\sigma_c/\gamma_{2t}$  in Eq. (4.17) contributes to the asymptotic tricritical exponent.

The model equations (3.3) do not adequately describe the competition between an isotropic (Heisenberg) fixed point and an anisotropic (Ising) fixed point. First, we have neglected the ("singular") shift of the critical temperature,<sup>14</sup>

$$[T_c(\mu_2) - T_c(0)]_{\text{sing}} = D\mu_2^{1/\phi_t} + \dots \quad (7.21)$$

This nonanalytic shift of  $T_c$  has important consequences here because for  $\phi_t > 0$  the role of the scaling fields  $\mu_1$  and  $\mu_2$  is interchanged. (The field  $\mu_2$  is conjugate to the most relevant scaling density  $Q_2$ , and  $\mu_1$  is the tangent to the critical line.) Depending on the value of  $D$  the "tricritical" path  $\mu_2 = \gamma\mu_1$  can lead to three different sets of asymptotic exponents. When  $D > 0$  then the path  $\mu_2 = \gamma\mu_1$  crosses the critical line before reaching the tricritical fixed point. Consequently the exponents are critical-line exponents. For  $D < 0$  the most relevant scaling density  $Q_2$  determines the tricritical exponent  $\gamma$ , which becomes  $\gamma_{2t} = 2/\gamma_{2t}$  (that is,  $\gamma_{2t} = \gamma_t/\phi_t$ ). In this section we have discussed the boundary case  $D = 0$ , which yields the asymptotic tricritical exponent  $\tilde{\gamma}$  of Eq. (7.18a). Second, because of the higher symmetry of the isotropic (Heisenberg) fixed point compared to the tricritical fixed point we expect that for the former case the parameter  $\gamma$  in Eq. (3.21) vanishes. Then the amusing dependence of  $\gamma_t$  on the value of  $D$  in Eq. (7.21) does not occur.

### VIII. SUMMARY

We have presented a scaling-field approach to crossover phenomena near critical points. In par-

ticular, scaling functions and effective critical exponents have been calculated.

Our approach differs from other formulations in three important aspects:

(i) It is based on a description of critical phenomena in terms of *scaling fields*. These fields are determined by a set of coupled, nonlinear differential equations. The specification of the initial conditions amounts to the specification of all interaction parameters and of the values of all experimental fields. The differential equations determine the "flow diagram" for the transition in the scaling-field space.

(ii) The approach extends the description of critical phenomena into the *whole critical region*. Approximations can be made in a controlled way by truncating the scaling-field equations. The guidance for approximations is a classification of the scaling fields according to their relevance. Crossover phenomena (including "confluent singularities," corrections to scaling, etc.) are described by nonlinear terms in the scaling-field equations.

(iii) The approach is based on a *microscopic description*. The renormalization-group procedure allows the derivation of the scaling-field equations from a Hamiltonian description of the problem. An example of such a derivation was given in our paper on "logarithmic corrections."

In the present article we have used as a starting point a simplified set of scaling-field equations for crossover phenomena. On this basis we have outlined the scaling-field theory for crossover effects. The model equations are constructed such as to contain the essential features of crossover phenomena. However, it is obvious from the approximations made that model Hamiltonians for various systems exhibiting crossover phenomena will lead to specific modifications of the equations. Further work on this aspect of the problem is under way.

### ACKNOWLEDGMENTS

The authors acknowledge with thanks the hospitality of the Institut für Festkörperforschung of the Kernforschungsanlage Jülich (E. K. R.) and of the Department of Physics at Duke University (F. J. W.). One of the authors (E. K. R.) is indebted to Professor H. Meyer for extensive discussions on the experimental aspects of tricritical phenomena, which were a considerable stimulus for these investigations.

### APPENDIX A: ASHKIN-TELLER MODEL

We note that the Hamiltonian (3.5) has a special symmetry for  $\bar{x} = 1$  which becomes obvious if we introduce  $S_i T_i = U_i$ . Then  $H$  is symmetric in the three variables  $S, T, U$ ,

$$H = -K \sum_{\langle i,j \rangle} (S_i S_j + T_i T_j + U_i U_j), \quad (\text{A1})$$

with the symmetric restriction

$$S_i T_i U_i = 1. \quad (\text{A2})$$

At first glance the Hamiltonian (A1) looks similar to the Hamiltonian of a classical Heisenberg model (three-vector model). However, the restriction (A2) leads to an effective interaction of the type  $STU$  which is a relevant operator for the fixed point of the three-vector model. [The operator was denoted by  $0f$  in Ref. 25. We found  $y = 1 - \epsilon/22 + O(\epsilon^2)$  for  $d = 4 - \epsilon$ .] If the fixed point of the Hamiltonian (A1) can be described at all by an expansion starting from the Gaussian fixed point then we expect an expansion around the dimension  $d = 6$  similar to Mack's.<sup>42</sup> From high-temperature expansions one estimates  $\gamma = 0.91$ .<sup>18</sup>

It is questionable whether this fixed point applies to the critical behavior for  $0 < \bar{x} < 1$  since we do not know whether the perturbation  $S_i S_j + T_i T_j - 2U_i U_j$ , which leads from  $\bar{x} = 1$  to  $\bar{x} < 1$ , is relevant or not. It can be shown that this perturbation is marginal (that is  $y = 0$ ) for the two-dimensional Ashkin-Teller model, where this result follows via duality<sup>12</sup> from the eight-vertex model.<sup>43</sup> If there exists an additional fixed point for the critical behavior in the region  $0 < \bar{x} < 1$  then we have to choose  $\bar{x}^*$  such that the perturbation by the slow transient  $Q_{2c}$  vanishes. A good estimation for  $y_c$  is then obtained from high-temperature expansion for  $\bar{x} = \bar{x}^*$ . We note that such a choice will not substantially affect our results.

One may argue along the lines sketched by Wilson and Fisher<sup>26</sup> that the system behaves like an  $XY$ -model along the critical line, which would imply  $\gamma_c = 1.32$ . However, since the exponents obtained by Ditzian<sup>18</sup> are quite different from this  $\gamma_c$ , we tend to assume that the Ashkin-Teller model is governed by a different fixed point.

#### APPENDIX B: GENERALIZED SCALING-FIELD EQUATIONS

Here we generalize the set of scaling-field equations (3.3) to describe a system exhibiting a crit-

ical line that is nonanalytic at the tricritical point. We keep Eq. (3.3c) but replace Eq. (3.3a) by

$$\begin{aligned} \frac{\partial \mu_1}{\partial l} = & y_{1t} \mu_1 (1 - \mu_2) + y_{1c} (\mu_1 - \mu_{1c}^*) \mu_2 \\ & + a \mu_2 (1 - \mu_2). \end{aligned} \quad (\text{B1})$$

This equation describes a system with fixed points at

$$(\mu_1^*, \mu_2^*) = \begin{cases} (0, 0), & \text{tricritical fixed point} \\ (\mu_{1c}^*, 1), & \text{critical fixed point.} \end{cases} \quad (\text{B2})$$

Near the tricritical fixed point we find, in linear order in  $\mu_i$ ,

$$\frac{\partial \mu_1}{\partial l} = y_{1t} \mu_1 + a \mu_2, \quad (\text{B3a})$$

$$\frac{\partial \mu_2}{\partial l} = y_{2t} \mu_2. \quad (\text{B3b})$$

The eigenvalues are  $y_{1t}$  and  $y_{2t}$ , the eigenvectors are  $(1, 0)$  and  $(a, y_{2t} - y_{1t})$ . For the critical fixed point the linearized equations read

$$\begin{aligned} \frac{\partial \mu_1}{\partial l} = & y_{1c} (\mu_1 - \mu_{1c}^*) \\ & - (y_{1t} \mu_{1c}^* + y_{1c} \mu_{1c}^* + a) (\mu_2 - 1), \end{aligned} \quad (\text{B4a})$$

$$\frac{\partial \mu_2}{\partial l} = -y_{2t} (\mu_2 - 1). \quad (\text{B4b})$$

The eigenvalues are  $y_{1c}$  and  $-y_{2t}$ , and the eigenvectors are  $(1, 0)$  and  $(y_{1t} \mu_{1c}^* + y_{1c} \mu_{1c}^* + a, y_{1c} + y_{2t})$ . We note that for  $y_{2t} = y_{1t}$  there is only one eigenvector at the tricritical fixed point. Similarly, for  $y_{1c} = -y_{2t}$ , only one eigenvector would exist at the critical fixed point. However, we have excluded this case by requiring  $y_{1c} > 0$ , and  $y_{2t} > 0$ .

Since Eq. (B1) is linear in  $\mu_1$  it can be integrated. We divide Eq. (B1) by Eq. (3.3c) and find for  $\mu_1$  as a function of  $\mu_2$

$$\begin{aligned} \mu_1(\mu_2) = & C_t \mu_2^{p_t} (1 - \mu_2)^{p_c} + \frac{p_c \mu_{1c}^*}{2 - p_t} \mu_2^2 (1 - \mu_2)^{p_c} F(1 + p_c, 2 - p_t; 3 - p_t; \mu_2) \\ & + \frac{a/y_{2t}}{1 - p_t} \mu_2 (1 - \mu_2)^{p_c} F(p_c, 1 - p_t; 2 - p_t; \mu_2), \end{aligned} \quad (\text{B5})$$

or

$$\begin{aligned} \mu_1(\mu_2) = & C_c \mu_2^{p_t} (1 - \mu_2)^{p_c} + \mu_{1c}^* \mu_2^{p_t} F(p_t - 1, -p_c; 1 - p_c; 1 - \mu_2) \\ & - \frac{a/y_{2t}}{1 - p_c} \mu_2^{p_t} (1 - \mu_2) F(p_t, 1 - p_c; 2 - p_c; 1 - \mu_2). \end{aligned} \quad (\text{B6})$$

Here the  $p$ 's denote the inverse crossover exponents,

$$p_t = y_{1t}/y_{2t}, \quad p_c = -y_{1c}/y_{2t}. \quad (\text{B7})$$

$F$  is the hypergeometric function,<sup>44</sup> and  $C_t$  and  $C_c$  are integration constants.<sup>31</sup> Equation (B5) is useful for the discussion close to the tricritical fixed point and Eq. (B6) for the discussion close to the critical fixed point. The connection between  $C_t$  and  $C_c$  is

$$C_t - C_c = \frac{\Gamma(1-p_c)\Gamma(1-p_t)}{\Gamma(2-p_c-p_t)} \times \left( \mu_{1c}^* (1-p_t) - \frac{a}{y_{2t}} \right). \quad (\text{B8})$$

We note that  $F(a, b; c; x)$  is analytic for  $|x| < 1$  provided  $c$  neither vanishes nor is a negative integer. Furthermore, for  $x=0$ ,  $F(a, b; c; 0)=1$ . From Eq. (B6) we see that only the curve with  $C_c = 0$  passes through the critical fixed point (note that  $p_c < 0$ ). This curve is the critical line. It is analytic at the critical fixed point. At the tricritical fixed point  $\mu_2 = 0$  and only the first term on the right-hand side of Eq. (B5) is nonanalytic, *provided*  $p_t$  is not a positive integer. Then the singular contribution to the equation for the critical line is

$$\mu_{1,\text{sing}} = C_t \mu_2^{p_t} + O(\mu_2^{p_t+1}). \quad (\text{B9})$$

When  $p_t = 1, 2, 3, \dots$ , i. e., when  $y_{1t} = y_{2t}, 2y_{2t}, 3y_{2t}, \dots$ , one finds

$$\mu_{1,\text{sing}} \propto \mu_2^{p_t} |\ln |\mu_2||. \quad (\text{B10})$$

When on the other hand  $p_t = 2 - p_c, 3 - p_c, \dots$ , i. e., when  $y_{1t} = 2y_{2t} + y_{1c}, 3y_{2t} + y_{1c}, \dots$ , or when  $\mu_{1c}^* (1 - p_t) = a/y_{2t}$ , then the amplitude  $C_t$  in Eq. (B9) vanishes.

The solutions (B5) and (B6) can be expressed in terms of the  $g$  scaling fields  $g_{it}(l)$  or  $g_{ic}(l)$  introduced in Eqs. (3.9) and (3.12). We define

$$C_t = g_{1t}(l)[g_{2t}(l)]^{-p_t}, \quad C_c = g_{1c}(l)[g_{2c}(l)]^{-p_c}. \quad (\text{B11})$$

Instead of Eqs. (3.8a) and (3.11a) we then obtain

$$\begin{aligned} \mu_1(l) = & g_{1t}(l)[1 + g_{2t}(l)]^{-(p_c + p_t)} \\ & + \frac{p_c \mu_{1c}^*}{2 - p_t} \frac{g_{2t}^2(l)}{1 + g_{2t}(l)} F(1 + p_c, 1; 3 - p_t; -g_{2t}(l)) \\ & + \frac{a/y_{2t}}{1 - p_t} \frac{g_{2t}(l)}{1 + g_{2t}(l)} F(p_c, 1; 2 - p_t; -g_{2t}(l)) \end{aligned} \quad (\text{B12})$$

and

$$\begin{aligned} \mu_1(l) = & g_{1c}(l)[1 + g_{2c}(l)]^{-(p_c + p_t)} \\ & + \frac{\mu_{1c}^*}{1 + g_{2c}(l)} F(p_t - 1, 1; 1 - p_c; -g_{2c}(l)) \\ & - \frac{a/y_{2t}}{1 - p_c} \frac{g_{2c}(l)}{1 + g_{2c}(l)} F(p_t, 1; 2 - p_c; -g_{2c}(l)). \end{aligned} \quad (\text{B13})$$

These results together with Eqs. (3.8b) and (3.11b), respectively, represent the  $l$ -dependent scaling fields on which further discussion can be based, as in Sec. III B.

\*Work supported in part by the National Science Foundation through Grant No. GH-36882.

<sup>1</sup>M. E. Fisher, Rep. Prog. Phys. **30**, 615 (1967).

<sup>2</sup>A preliminary report on this work was presented at the Conference on the Renormalization Group in Critical Phenomena and Quantum Field Theory, Temple University, Philadelphia, Pa., 1973 (unpublished).

<sup>3</sup>K. G. Wilson, Phys. Rev. B **4**, 3184 (1971).

<sup>4</sup>F. J. Wegner, Phys. Rev. B **5**, 4529 (1972).

<sup>5</sup>For a review of the renormalization-group theory and further references see K. G. Wilson and J. B. Kogut, Phys. Rep. (to be published).

<sup>6</sup>E. K. Riedel and F. J. Wegner, Phys. Rev. Lett. **29**, 349 (1972).

<sup>7</sup>F. J. Wegner and E. K. Riedel, Phys. Rev. B **7**, 248 (1973).

<sup>8</sup>R. Bidaux, P. Carrara, and B. Vivet, J. Phys. Chem. Solids **28**, 2453 (1967).

<sup>9</sup>M. Blume, V. J. Emery, and R. B. Griffiths, Phys. Rev. A **4**, 1071 (1971).

<sup>10</sup>J. Ashkin and E. Teller, Phys. Rev. **64**, 178 (1943).

<sup>11</sup>Compare also the formulation of the Ashkin-Teller model by C. Fan, Phys. Rev. Lett. **29**, 158 (1972), and Ref. 12.

<sup>12</sup>F. J. Wegner, J. Phys. C **5**, L131 (1972).

<sup>13</sup>M. E. Fisher, Phys. Rev. **176**, 257 (1968).

<sup>14</sup>E. Riedel and F. Wegner, Z. Phys. **225**, 195 (1969);

Phys. Rev. Lett. **24**, 730 (1970); **24**, 930 (E) (1970).

<sup>15</sup>E. K. Riedel, J. Appl. Phys. **42**, 1383 (1971).

<sup>16</sup>See also the review in M. E. Fisher and D. M. Jasnow, *Theory of Correlations in the Critical Region* (Academic, New York, to be published).

<sup>17</sup>E. K. Riedel, Phys. Rev. Lett. **28**, 675 (1972).

<sup>18</sup>R. V. Ditzian, Phys. Lett. A **42**, 67 (1972).

<sup>19</sup>M. E. Fisher and P. E. Scesney, Phys. Rev. A **2**, 825 (1970).

<sup>20</sup>F. J. Wegner and A. Houghton, Phys. Rev. A **8**, 401 (1973).

<sup>21</sup>Scaling fields have been introduced in the phenomenological scaling theory of Ref. 17. The fact that the critical line near a tricritical point defines a special direction in the experimental field space made it necessary to introduce generalized scaling variables. The significance of the direction of approach to criticality for the values of critical exponents had been pointed out by Griffiths and Wheeler [Phys. Rev. A **2**, 1047 (1970)]. Wegner (Ref. 4) was the first to show that the renormalization-group procedure yields a microscopic definition of generalized scaling variables. A renormalization-group approach to tricritical phase transitions was subsequently proposed by the authors in Refs. 6 and 7. These investigations show that all phase transitions determine a frame of reference of scaling fields which is related to special geometrical features of the corre-

sponding phase diagrams. Tricritical phase transitions are an example where the scaling fields are *not* proportional to the deviating experimental fields, which consequently are not the correct scaling variables. The dependence of the scaling fields on the experimental fields implies, for example, that near tricritical points the nonordering density exhibits weak ( $\alpha$ -type) induced critical fluctuations at the critical line in the  $(T, G)$  plane and even strong ( $\gamma$ -type) induced fluctuations at the critical lines that bound the first-order transition wings.

<sup>22</sup>Equation (XI. 17) of Ref. 5 has group properties, whereas Eq. (2. 20) of Ref. 20 has only semigroup properties. We suggest that the basic equation  $H_t = R^l H_0$  be termed the *Wilson equation*. Wilson (Ref. 3) was the first to derive an explicit expression for the renormalization-group operator  $R^l$ .

<sup>23</sup>From Eqs. (B16) to (B18) of Ref. 7 one obtains in the limit  $l \rightarrow 0$  and  $l' \rightarrow l$  the equation of motion (2. 7).

<sup>24</sup>M. Wortis, Newport Beach Conference on Phase Transitions, 1970 (unpublished).

<sup>25</sup>F. J. Wegner, Phys. Rev. B 6, 1891 (1972).

<sup>26</sup>K. G. Wilson and M. E. Fisher, Phys. Rev. Lett. 28, 240 (1972).

<sup>27</sup>L. P. Kadanoff and F. J. Wegner, Phys. Rev. B 4, 3989 (1971).

<sup>28</sup>The exponents  $\nu \approx 0.645$  and  $\eta \approx \frac{1}{18}$  from series expansions, which do not satisfy the scaling relation  $2 - \alpha = d\nu$ , lead to  $y_{1t} = 1.55$  and  $y_{2t} = 0.1$ . With these exponents the width of the 25% crossover region becomes, by about a factor of  $7 \times 10^8$ , larger than the corresponding width for a system with the exponents (3. 6).

<sup>29</sup>For  $\mu_2$  outside the interval  $[0, 1]$  the boundary condition (3. 31) for  $\chi$  is not defined for all values of  $\mu_1 > 0$  and  $\mu_2$ .

<sup>30</sup>The second factor in the expressions for the scaling functions  $\nu$  is *universal*, with the parameters of the system entering *only* through the scaling fields. The first factor  $\bar{\chi}$ , which remains undetermined in our theory for the critical region, reflects properties of

the system in the *noncritical* region and can be taken from experiments or calculations therein.

<sup>31</sup>The quantity  $C$  defined by Eq. (4. 5) is equal to  $C_c$  and  $C_t$  introduced in Appendix B if  $a = 0$  and  $\mu_{1c}^* = 0$ .

<sup>32</sup>If additional scaling fields would have been taken into account, we would have found that the scaling results are only valid under the further condition  $\mu_1 \ll 1$ .

<sup>33</sup>K. G. Wilson, Phys. Rev. Lett. 28, 548 (1972).

<sup>34</sup>The domain of a fixed point has been defined in Ref. 5 as the set of initial states with trajectories approaching that fixed point. Hence the domain of the critical fixed point consists of all points on the critical surface, whereas the domain of the tricritical fixed point consists only of that point.

<sup>35</sup>See also F. Wegner and E. Riedel, J. Phys. (Paris) 32, C1-519 (1971), Eq. (3. 5).

<sup>36</sup>In Eqs. (6. 4) and (6. 5) we did not indicate any implicit factors of  $1/k_B T$ , etc.

<sup>37</sup>L. P. Kadanoff, in *Proceedings of the International School of Physics "Enrico Fermi," Varenna, 1970*, edited by M. S. Green (Academic, New York, 1971), p. 100.

<sup>38</sup>Extrapolation techniques allow the extraction of the true asymptotic critical exponent only if the convergence of the effective exponent  $\gamma_{eff}(\nu)$  is sufficiently good. (Compare also Fig. 14.)

<sup>39</sup>In Eq. (7. 15) we have omitted the  $(\partial \ln \bar{\chi} / \partial \hat{\mu}_2)$  term.

<sup>40</sup>M. E. Fisher and P. Pfeuty, Phys. Rev. B 6, 1889 (1972); and P. Pfeuty, M. E. Fisher, and D. Jasnow, AIP Conf. Proc. 10, 817 (1973).

<sup>41</sup>D. Jasnow and M. Wortis, Phys. Rev. 176, 739 (1968).

<sup>42</sup>G. Mack (report of work prior to publication).

<sup>43</sup>R. J. Baxter, Phys. Rev. Lett. 26, 832 (1971); Ann. Phys. (N. Y.) 70, 193 (1972).

<sup>44</sup>*Handbook of Mathematical Functions*, edited by M. Abramowitz and I. A. Stegun (Natl. Bur. Std. Appl. Math. Series, No. 55) (U.S. GPO Washington, D. C., 1965), Chap. 15.